CAR-TR-780
CS-TR-3502
July 1995

DACA76-92-C-0009
N00014-93-1-0257
IRI-90-57934

Directions of motion fields are hardly ever ambiguous

Tomas Brodsky
Cornelia Fermüller
Yiannis Aloimonos

Computer Vision Laboratory
Center for Automation Research
University of Maryland
College Park, MD 20742-3275

COMPUTER VISION LABORATORY

CENTER FOR AUTOMATION RESEARCH

UNIVERSITY OF MARYLAND
COLLEGE PARK, MARYLAND
20742-3275

CAR-TR-780
CS-TR-3501
July 1995

DACA76-92-C-0009
N00014-93-1-0257
IRI-90-57934

Directions of motion fields are hardly ever ambiguous

Tomas Brodsky
Cornelia Fermüller
Yiannis Aloimonos

Computer Vision Laboratory
Center for Automation Research
University of Maryland
College Park, MD 20742-3275

Abstract

If instead of the full motion field, we consider only the direction of the motion field due to a rigid motion, what can we say about the three-dimensional motion information contained in it? This paper provides a geometric analysis of this question based solely on the constraint that the depth of the surfaces in view is positive.

It is shown that, considering as the imaging surface the whole sphere, independently of the scene in view, two different rigid motions cannot give rise to the same directional motion field. If we restrict the image to half of a sphere (or an infinitely large image plane) two different rigid motions with instantaneous translational and rotational velocities $(\mathbf{t}_1, \boldsymbol{\omega}_1)$ and $(\mathbf{t}_2, \boldsymbol{\omega}_2)$ cannot give rise to the same directional motion field unless the plane through $\mathbf{t}_1$ and $\mathbf{t}_2$ is perpendicular to the plane through $\boldsymbol{\omega}_1$ and $\boldsymbol{\omega}_2$ (i.e., $(\mathbf{t}_1 \times \mathbf{t}_2) \cdot (\boldsymbol{\omega}_1 \times \boldsymbol{\omega}_2) = 0$). In addition, in order to give practical significance to these uniqueness results for the case of a limited field of view, we also characterize the locations on the image where the motion vectors due to the different motions must have different directions.

If $(\boldsymbol{\omega}_1 \times \boldsymbol{\omega}_2) \cdot (\mathbf{t}_1 \times \mathbf{t}_2) = 0$ and certain additional constraints are met, then the two rigid motions could produce motion fields with the same direction. For this to happen the depth of each corresponding surface has to be within a certain range, defined by a second and a third order surface. Finally, as a byproduct of the analysis it is shown that if we also consider the constraint of positive depth the full motion field on a half sphere uniquely constrains 3D motion independently of the scene in view.

The support of the Advanced Research Projects Agency (ARPA Order No. 8459) and the U.S. Army Topographic Engineering Center under Contract DACA76-92-C-0009, the Office of Naval Research under Contract N00014-93-1-0257, National Science Foundation under Grant IRI-90-57934, , and the Austrian "Fonds zur Förderung der wissenschaftlichen Forschung", project No. S 7003, is gratefully acknowledged.

1 Introduction and Motivation

The basis of the majority of visual motion studies has been the motion field, i.e., the projection of the velocities of 3D scene points on the image. Classical results on the uniqueness of motion fields [6, 9, 10] as well as displacement fields [8, 12, 14] have formed the foundation of most research on rigid motion analysis that addressed the 3D motion problem by first approximating the motion field through the optical flow and then interpreting the optical flow to obtain 3D motion and structure [2, 7, 13, 15].

The difficulties involved in the estimation of optical flow have recently given rise to a small number of studies considering as input to the visual motion interpretation process some partial optical flow information. In particular the projection of the optical flow on the gradient direction, the so-called normal flow [5, 11], and the projections of the flow on different directions [1, 3] have been utilized. In [3] constraints on the sign of the projection of the flow on various directions were presented. These constraints on the sign of the flow were derived using only the rigid motion model, with the only constraint on the scene being that the depth in view has to be positive at every point—the so-called "depth-positivity" constraint. In the sequel we are led naturally to the question of what these constraints, or more generally any constraint on the sign of the flow, can possibly tell us about three-dimensional motion and the structure of the scene in view. Thus we would like to investigate the amount of information in the sign of the projection of the flow. Since knowing the sign of the projection of a motion vector in all directions is equivalent to knowing the direction of the motion vector, our question amounts to studying the relationship between the directions of 2D motion vectors and 3D rigid motion.

We next state the well-known equation for rigid motion for the case of a spherical imaging surface. We describe the constraints and discuss the information exploited when using the full flow as opposed to the information employed when using only the direction of flow. As will be shown, whereas full flow allows for derivation of the direction of translation and the complete rotation, from the orientation of the flow only the direction of translation and the direction of rotation can be obtained.

The 2D motion field on the imaging surface is the projection of the 3D motion field of

the scene points moving relative to that surface. Suppose the observer is moving rigidly with instantaneous translation $\mathbf{t} = (U, V, W)$ and instantaneous rotation $\boldsymbol{\omega} = (\alpha, \beta, \gamma)$ (see Figure 1); then each scene point $\mathbf{R} = (X, Y, Z)$ measured with respect to a coordinate system $OXYZ$ fixed to the camera moves relative to the camera with velocity $\dot{\mathbf{R}}$, where

$$\dot{\mathbf{R}} = -\mathbf{t} - \boldsymbol{\omega} \times \mathbf{R}$$

If the center of projection is at the origin and the image is formed on a sphere with radius 1, the relationship between the image point $\mathbf{r}$ and the scene point $\mathbf{R}$ under perspective projection is

$$\mathbf{r} = \frac{\mathbf{R}}{|\mathbf{R}|}$$

with $|\mathbf{R}|$ being the norm of the vector $\mathbf{R}$.

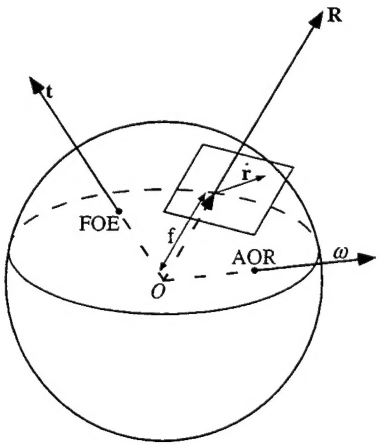

Figure 1: Image formation on a spherical retina under perspective projection.

If we now differentiate $\mathbf{r}$ with respect to time and substitute for $\dot{\mathbf{R}}$, we obtain the following equation for $\dot{\mathbf{r}}$:

$$\dot{\mathbf{r}} = v_{\mathrm{tr}}(\mathbf{r}) + v_{\mathrm{rot}}(\mathbf{r}) = \frac{1}{|\mathbf{R}|}((\mathbf{t} \cdot \mathbf{r})\mathbf{r} - \mathbf{t}) - \boldsymbol{\omega} \times \mathbf{r} = -\frac{1}{|\mathbf{R}|}(\mathbf{r} \times (\mathbf{t} \times \mathbf{r})) - \boldsymbol{\omega} \times \mathbf{r}$$

The first term $v_{\mathrm{tr}}(\mathbf{r})$ corresponds to the translational component which depends on the depth $Z = |\mathbf{R}|$, the distance of $\mathbf{R}$ to the center of projection. The direction of $v_{\mathrm{tr}}(\mathbf{r})$ is along great circles (longitudes) pointing away from the Focus of Expansion ($\mathbf{t}$) and towards the Focus of Contraction ($-\mathbf{t}$). The second term $v_{\mathrm{rot}}(\mathbf{r})$ corresponds to the rotational component which

is independent of depth. Its direction is along latitudes around the axis of rotation (counterclockwise around ω and clockwise around $-\omega$). See Figure 2a, b and c for translational, rotational, and general motion fields on the sphere.

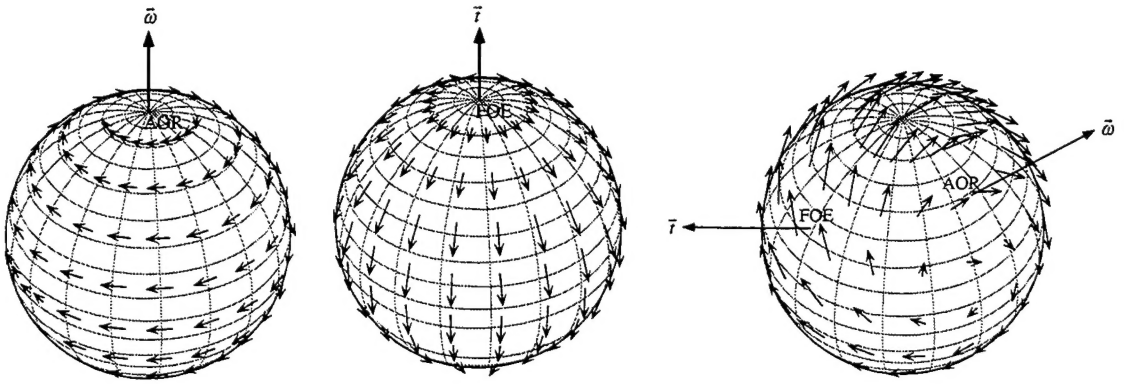

(a) (b) (c)

Figure 2: Example of (a) a rotational, (b) a translational, (c) a general motion field on a sphere.

As can be seen, without additional constraints there is an ambiguity in the computation of shape and translation. It is not possible to disentangle the effects of $\mathbf{t}$ and $|\mathbf{R}|$, and thus we can only derive the direction of translation. If all we have is the direction of the flow we can project $\dot{\mathbf{r}}$ on any unit vector $\mathbf{n}_i$ on the image and obtain an inequality constraint:

$$\dot{\mathbf{r}} \cdot \mathbf{n}_i = \left(\frac{1}{|\mathbf{R}|}((\mathbf{t} \cdot \mathbf{r})\mathbf{r} - \mathbf{t}) - \boldsymbol{\omega} \times \mathbf{r} \right) \cdot \mathbf{n}_i > 0 \quad \text{or} \quad < 0$$

From this inequality we certainly cannot recover the magnitude of translation, since the optical flow already does not allow us to compute it.

In addition we are also restricted in the computation of the rotational parameters. If we multiply $\boldsymbol{\omega}$ by a positive constant, leave $\mathbf{t}$ fixed, but multiply $\frac{1}{|\mathbf{R}|}$ by the same positive constant, the sign of the flow is not affected. Thus from the direction of the flow we can at most compute the axis of rotation and, as discussed before, the axis of translation. Hereafter, for the sake of brevity, we will refer to the motion field also as the flow field or simply flow, and to the direction of the motion field as the directional flow field or simply directional flow.

2 Relationship Between the Orientation of the Flow and the Depth-positivity Constraint

If we have the flow $\dot{\mathbf{r}}$, we know the value of the projection of $\dot{\mathbf{r}}$ on any direction and we set all the possible information by choosing two directions $\mathbf{n}_1$ and $\mathbf{n}_2$ (usually orthogonal). Thus we have

$$\dot{\mathbf{r}} \cdot \mathbf{n}_i = \frac{1}{|\mathbf{R}|}((\mathbf{t} \cdot \mathbf{r})\mathbf{r} - \mathbf{t}) \cdot \mathbf{n}_i - (\boldsymbol{\omega} \times \mathbf{r}) \cdot \mathbf{n}_i \qquad \text{for} \qquad i = 1, 2 \tag{1}$$

We can solve equation (1) for the depth,

$$\frac{\dot{\mathbf{r}} \cdot \mathbf{n}_i + (\boldsymbol{\omega} \times \mathbf{r}) \cdot \mathbf{n}_i}{((\mathbf{t} \cdot \mathbf{r})\mathbf{r} - \mathbf{t}) \cdot \mathbf{n}_i} = \frac{1}{|\mathbf{R}|} \qquad \text{for} \qquad i = 1, 2$$

Knowing the value in both directions $\mathbf{n}_1$ and $\mathbf{n}_2$ we know that the inverse depth has to be the same, and also has to be positive; thus

$$\frac{\dot{\mathbf{r}} \cdot \mathbf{n}_1 + (\boldsymbol{\omega} \times \mathbf{r}) \cdot \mathbf{n}_1}{((\mathbf{t} \cdot \mathbf{r})\mathbf{r} - \mathbf{t}) \cdot \mathbf{n}_1} = \frac{\dot{\mathbf{r}} \cdot \mathbf{n}_2 + (\boldsymbol{\omega} \times \mathbf{r}) \cdot \mathbf{n}_2}{((\mathbf{t} \cdot \mathbf{r})\mathbf{r} - \mathbf{t}) \cdot \mathbf{n}_2} > 0$$

If on the other hand we do not use the value of the flow but only its direction and thus the sign of the projection of the flow on $\mathbf{n}_i$, then the only constraint that can be utilized is the inequality, which comes from the fact that the depth is positive. Using only the orientation of the flow we obtain for every direction $\mathbf{n}_i$:

$$\frac{\dot{\mathbf{r}} \cdot \mathbf{n}_i + (\boldsymbol{\omega} \times \mathbf{r}) \cdot \mathbf{n}_i}{((\mathbf{t} \cdot \mathbf{r})\mathbf{r} - \mathbf{t}) \cdot \mathbf{n}_i} > 0$$

This inequality provides inequality constraints on the rotational and translational components, which are independent of the scene: If we consider the sign of the translational component $((\mathbf{t} \cdot \mathbf{r})\mathbf{r} - \mathbf{t}) \cdot \mathbf{n}_i$ and the sign of the rotational component $(\boldsymbol{\omega} \times \mathbf{r}) \cdot \mathbf{n}_i$ and assume that each of them is either positive or negative, there are $2 \times 2 = 4$ combinations of signs. But once we know the sign of the flow $\dot{\mathbf{r}} \cdot \mathbf{n}_i$, one of these four combinations is no longer possible. This observation has been used in the development of global constraints for 3D motion estimation. Choosing directions $\mathbf{n}_i$ in particular ways the signs of $(\dot{\mathbf{r}} \cdot \mathbf{n}_i)$ form global patterns of positive and negative areas on the image [3–5]. These patterns, whose location and form encodes information about 3D motion, were successfully used in the recovery of egomotion. In this paper, by pursuing a theoretical investigation of the amount of information present in directional flow fields, we demonstrate the power of the qualitative image

measurements already used empirically, and justify their utilization in global constraints for three-dimensional dynamic vision problems.

The organization of this paper is as follows: In Section 3 we develop the preliminaries—constraints that will be used in the uniqueness analysis. Given two rigid motions, we study what the constraints are on the surfaces in view for the two motion fields to have the same direction at every point. From these constraints, we investigate for which points of the image one of the surfaces must have negative depth. The locations where negative depth occurs are described implicitly in the form of constraints on the signs of functions depending on the image coordinates and the two three-dimensional motions. The existence of image points whose associated depth is negative ensures that the two rigid motions cannot produce motion fields with the same direction. In Section 4, which contains the main uniqueness proof, we study conditions under which two rigid flow fields could have the same direction at every point on a half sphere (i.e., conditions under which there do not exist points of negative depth), and we visualize the locations of negative depth on the sphere. Section 5 is devoted to the treatment of special cases. As a byproduct of the analysis, in Section 6 we investigate the ambiguity of rigid motion for full flow assuming that depth has to be positive, and show that any two different motions can be distinguished on a hemispherical image from full flow. Section 7 summarizes the results. Appendix A studies whether more than two rigid motions could produce the same directional flow field, and the rest of the Appendices (B–F) describe and prove a number of geometric properties used in the main part of the paper.

3 Critical Surface Constraints

Let us assume that two different rigid motions yield the same direction of flow at every point in the image. Let $\mathbf{t}_1$ and $\boldsymbol{\omega}_1$ be translational and rotational velocities of the first motion, and let $\mathbf{t}_2$ and $\boldsymbol{\omega}_2$ be translational and rotational velocities of the second motion. Since from the direction of flow we can only recover the directions of the translation and rotation axes, we assume all four vectors $\mathbf{t}_1$, $\mathbf{t}_2$, $\boldsymbol{\omega}_1$ and $\boldsymbol{\omega}_2$ to be of unit length. Let $Z_1(\mathbf{r})$ and $Z_2(\mathbf{r})$ be the functions, mapping points $\mathbf{r}$ on the image into the real numbers, that represent the depths of the surfaces in view corresponding to the two motions. In the future we will refer to Z_1

and Z_2 as the two depth maps. In this section we investigate the constraints that must be satisfied by Z_1 and Z_2 in order for the two flow fields to have the same direction.

We assume that the two depths are positive, and allow Z_1 or Z_2 to be infinitely large. Thus we assume $1/Z_1 \geq 0$ and $1/Z_2 \geq 0$.

3.1 Notation

We start by defining some notation:

$$\begin{aligned} f_\omega(\mathbf{r}) &= [\boldsymbol{\omega}_1\, \boldsymbol{\omega}_2\, \mathbf{r}] \\ f_t(\mathbf{r}) &= [\mathbf{t}_1\, \mathbf{t}_2\, \mathbf{r}] \\ g_{ij}(\mathbf{r}) &= (\boldsymbol{\omega}_i \times \mathbf{r}) \cdot (\mathbf{t}_j \times \mathbf{r}) \quad \text{for } i, j = 1,2 \end{aligned} \tag{2}$$

where $[\mathbf{abc}] = (\mathbf{a} \times \mathbf{b}) \cdot \mathbf{c}$ denotes the triple product of vectors $\mathbf{a}$, $\mathbf{b}$ and $\mathbf{c}$.

These functions have a simple geometric meaning. If $\boldsymbol{\omega}_1 \times \boldsymbol{\omega}_2 = 0$, then $f_\omega(\mathbf{r}) = 0$ for any $\mathbf{r}$. If $\boldsymbol{\omega}_1 \times \boldsymbol{\omega}_2 \neq 0$, then $f_\omega(\mathbf{r})$ is zero for points $\mathbf{r}$ lying on a geodesic passing through $\boldsymbol{\omega}_1$ and $\boldsymbol{\omega}_2$. In this case $f_\omega(\mathbf{r}) = 0$ defines the locus of points $\mathbf{r}$ where $v_{\text{rot}_1}(\mathbf{r})$, the rotational component of the first motion, is parallel to $v_{\text{rot}_2}(\mathbf{r})$, the rotational component of the second motion. Similarly $f_t(\mathbf{r})$ is either zero everywhere, or it is zero for points lying on a geodesic passing through $\mathbf{t}_1$ and $\mathbf{t}_2$. In this case $f_t(\mathbf{r}) = 0$ is the locus of points $\mathbf{r}$ where $v_{\text{tr}_1}(\mathbf{r})$, the translational component of the first motion, is parallel to $v_{\text{tr}_2}(\mathbf{r})$, the translational component of the second motion.

If $\boldsymbol{\omega}_i = 0$, or $\mathbf{t}_j = 0$, then $g_{ij}(\mathbf{r}) = 0$ for any $\mathbf{r}$. If they are non-zero, then $g_{ij}(\mathbf{r})$ is zero at points lying on a second order curve consisting of two closed curves on the sphere, the so-called zero motion contour of motion $(\mathbf{t}_j, \boldsymbol{\omega}_i)$. Equation $g_{ij}(\mathbf{r}) = 0$ defines the locus of points where $v_{\text{rot}_i}(\mathbf{r})$ is parallel to $v_{\text{tr}_j}(\mathbf{r})$ (see Appendix B). Throughout the paper the functions $f_\omega(\mathbf{r})$, $f_t(\mathbf{r})$, $g_{ij}(\mathbf{r})$ and the curves defined by their zero crossings will play very important roles.

To simplify the notation we will usually drop $\mathbf{r}$ and write only f_i and g_{ij} where the index i in f_i can take values $\mathbf{t}$ and $\boldsymbol{\omega}$. There is a simple relationship between f_i and g_{ij}. Let

$$\mathbf{u}_1 = (\mathbf{r} \times (\mathbf{t}_1 \times \mathbf{r})) \times (\boldsymbol{\omega}_1 \times \mathbf{r}) = -[\boldsymbol{\omega}_1\, \mathbf{r}\, (\mathbf{t}_1 \times \mathbf{r})]\mathbf{r} = -g_{11}\, \mathbf{r}$$

$$\mathbf{u}_2 = (\mathbf{r} \times (\mathbf{t}_2 \times \mathbf{r})) \times (\boldsymbol{\omega}_2 \times \mathbf{r}) = -g_{22}\,\mathbf{r}$$

Since we assume $(\mathbf{r} \cdot \mathbf{r}) = 1$, we obtain

$$\mathbf{u}_1 \cdot \mathbf{u}_2 = g_{11}g_{22} \tag{3}$$

Let

$$\mathbf{u}_3 = (\mathbf{t}_2 \times \mathbf{r}) \times (\mathbf{r} \times (\boldsymbol{\omega}_2 \times \mathbf{r})) = -\mathbf{u}_2$$

Then

$$\mathbf{u}_1 \cdot \mathbf{u}_2 = -\mathbf{u}_1 \cdot \mathbf{u}_3 = f_t f_\omega + g_{12}g_{21} \tag{4}$$

From equations (3) and (4) we get

$$g_{11}g_{22} = f_t f_\omega + g_{12}g_{21} \tag{5}$$

3.2 Conditions for ambiguity

Assuming that motion $(\mathbf{t}_1, \boldsymbol{\omega}_1)$ with depth map Z_1 and motion $(\mathbf{t}_2, \boldsymbol{\omega}_2)$ with depth map Z_2 give rise to flow fields with the same direction at any point; then there exists $\mu > 0$ such that

$$-\frac{1}{Z_1}(\mathbf{r} \times (\mathbf{t}_1 \times \mathbf{r})) - \boldsymbol{\omega}_1 \times \mathbf{r} = \mu\,(-\frac{1}{Z_2}(\mathbf{r} \times (\mathbf{t}_2 \times \mathbf{r})) - \boldsymbol{\omega}_2 \times \mathbf{r}) \tag{6}$$

By projecting the vector equation (6) on directions $\mathbf{t}_2 \times \mathbf{r}$ and $\mathbf{r} \times (\boldsymbol{\omega}_2 \times \mathbf{r})$ we obtain two scalar equations

$$\frac{1}{Z_1}[\mathbf{t}_1\mathbf{t}_2\mathbf{r}] + (\boldsymbol{\omega}_1 \times \mathbf{r}) \cdot (\mathbf{t}_2 \times \mathbf{r}) = \mu\,(\boldsymbol{\omega}_2 \times \mathbf{r}) \cdot (\mathbf{t}_2 \times \mathbf{r}) \tag{7}$$

$$\frac{1}{Z_1}(\boldsymbol{\omega}_2 \times \mathbf{r}) \cdot (\mathbf{t}_1 \times \mathbf{r}) - [\boldsymbol{\omega}_1\boldsymbol{\omega}_2\mathbf{r}] = \mu\,\frac{1}{Z_2}(\boldsymbol{\omega}_2 \times \mathbf{r}) \cdot (\mathbf{t}_2 \times \mathbf{r}) \tag{8}$$

Since μ is positive, from (7) and (8) we get constraints on $\frac{1}{Z_1}$:

$$\mathrm{sgn}(\frac{1}{Z_1}f_t + g_{12}) = \mathrm{sgn}(g_{22}) \tag{9}$$

$$\mathrm{sgn}(\frac{1}{Z_1}g_{21} - f_\omega) = \mathrm{sgn}(\frac{1}{Z_2}g_{22}) \tag{10}$$

where $\mathrm{sgn}(\cdot)$ denotes the sign function.

Let us define $s_1 = -g_{12}/f_t$ and $s'_1 = f_\omega/g_{21}$. At any point, f_i and g_{ij} are constant, so equations (9) and (10) provide simple constraints on $\frac{1}{Z_1}$. We call them the s_1-constraint and the s'_1-constraint respectively.

Similarly we can project equation (6) on vectors $\mathbf{t}_1 \times \mathbf{r}$ and $\mathbf{r} \times (\boldsymbol{\omega}_1 \times \mathbf{r})$ and obtain constraints on $\frac{1}{Z_2}$:

$$\text{sgn}(g_{11}) = \text{sgn}(-\frac{1}{Z_2} f_t + g_{21}) \tag{11}$$

$$\text{sgn}(\frac{1}{Z_1} g_{11}) = \text{sgn}(\frac{1}{Z_2} g_{12} + f_\omega) \tag{12}$$

We define $s_2 = g_{21}/f_t$, $s'_2 = -f_\omega/g_{12}$. Equations (11) and (12) provide constraints on $\frac{1}{Z_2}$, and we thus call them the s_2-constraint and the s'_2-constraint.

Let us now interpret these constraints: $\frac{1}{Z_2}$ is always non-negative; thus, if the two motions $(\mathbf{t}_1, \boldsymbol{\omega}_1)$, $(\mathbf{t}_2, \boldsymbol{\omega}_2)$ with their corresponding depth maps Z_1 and Z_2 produce flow with the same direction, the depth Z_1 must satisfy

$$\begin{array}{lll} \text{either} & \frac{1}{Z_1} f_t + g_{12} > 0 \quad \text{and} & \frac{1}{Z_1} g_{21} - f_\omega \geq 0 \\ \text{or} & \frac{1}{Z_1} f_t + g_{12} < 0 \quad \text{and} & \frac{1}{Z_1} g_{21} - f_\omega \leq 0 \end{array}$$

Thus Z_1 has a relationship to the surfaces:

$$Z(\mathbf{r}) = \frac{1}{s_1(\mathbf{r})} \tag{13}$$

$$\text{and} \qquad Z(\mathbf{r}) = \frac{1}{s'_1(\mathbf{r})} \tag{14}$$

Equations (13) and (14) provide hybrid definitions of scene surfaces. To express the surfaces in scene coordinates $\mathbf{R}$, we substitute in the above equations $Z(\mathbf{r})\mathbf{r} = \mathbf{R}$. Dividing (13) by $Z(\mathbf{r})$ and replacing $Z(\mathbf{r})^2$ by $\mathbf{R}^2$ in (14) we obtain

$$(\mathbf{t}_1 \times \mathbf{t}_2) \cdot \mathbf{R} + (\boldsymbol{\omega}_1 \times \mathbf{R}) \cdot (\mathbf{t}_2 \times \mathbf{R}) = 0 \tag{15}$$

$$\text{and} \qquad (\boldsymbol{\omega}_2 \times \mathbf{R}) \cdot (\mathbf{t}_1 \times \mathbf{R}) - ((\boldsymbol{\omega}_1 \times \boldsymbol{\omega}_2) \cdot \mathbf{R})\mathbf{R}^2 = 0 \tag{16}$$

Thus we see that Z_1 is constrained through (15) by a second order surface and through (16) by a third order surface. At some points it has to be inside the first surface and at some points it has to be outside the first surface. In addition, at some points it has to be inside the

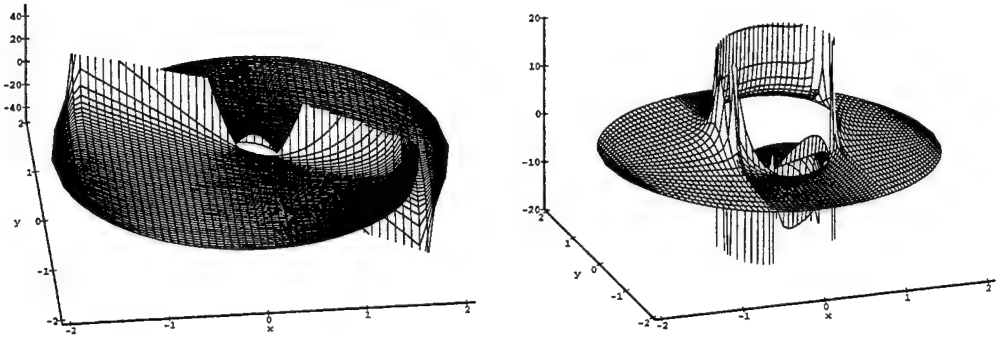

(a) (b)

Figure 3: Two rigid motions $(\mathbf{t}_1, \boldsymbol{\omega}_1)$, $(\mathbf{t}_2, \boldsymbol{\omega}_2)$ constrain the possible depth Z_1 of the first surface by a second and a third order surface. The particular surfaces shown in the coordinate system of the imaging sphere, projected stereographically, correspond to the motion configuration of Figure 7.

second surface and at some points it has to be outside the second surface. Figure 3 provides a pictorial description of the two surfaces constraining Z_1.

Analogous to the above derivation, from equations (11) and (12) we obtain a further second and third order surface pair, which constrain the depth map Z_2.

3.3 Interpretation of surface constraints

We next describe the s_1- and s_1'-constraints in detail. For convenience, we express these constraints for $\frac{1}{Z_1}$.

If $f_t = 0$, then the s_1-constraint is $\text{sgn}(g_{12}) = \text{sgn}(g_{22})$, i.e., it does not depend on Z_1. Thus it is either satisfied by any Z_1, or it cannot be satisfied by any Z_1.

If $f_t \neq 0$, then we get the s_1-constraint $\text{sgn}(\frac{1}{Z_1} - s_1) = \text{sgn}(g_{22})\text{sgn}(f_t)$. So the s_1-constraint is

- $\frac{1}{Z_1} > s_1$, if $\text{sgn}(g_{22})\,\text{sgn}(f_t) > 0$
- $\frac{1}{Z_1} = s_1$, if $\text{sgn}(g_{22}) = 0$
- $\frac{1}{Z_1} < s_1$, if $\text{sgn}(g_{22})\,\text{sgn}(f_t) < 0$

If $g_{21} = 0$, then the s_1'-constraint does not depend on Z_1.

If $g_{21} \neq 0$, we get $\text{sgn}(\frac{1}{Z_1} - s_1') = \text{sgn}(\frac{1}{Z_2} g_{22})\text{sgn}(g_{21})$. Since we assume $\frac{1}{Z_2} \geq 0$, $\text{sgn}(\frac{1}{Z_2} g_{22})$ is either 0, or $\text{sgn}(g_{22})$. So the s_1'-constraint is

- $\frac{1}{Z_1} \geq s_1'$, if $\text{sgn}(g_{22})\,\text{sgn}(g_{21}) > 0$
- $\frac{1}{Z_1} = s_1'$, if $\text{sgn}(g_{22}) = 0$
- $\frac{1}{Z_1} \leq s_1'$, if $\text{sgn}(g_{22})\,\text{sgn}(g_{21}) < 0$

At each point we have the additional constraint $\frac{1}{Z_1} \geq 0$. If all three constraints can be satisfied simultaneously at a point in the image, then there is an interval (bounded or unbounded) of values of Z_1 satisfying them. If the constraints cannot be satisfied, this means that the two flows at this point cannot have the same direction and we say that we have a *contradictory point.*

In the following table we summarize the three constraints on $\frac{1}{Z_1}$. According to the inequality relationships from the s_1-constraint and the s_1'-constraint we classify the image points into four categories (type I–IV). The table analyzes the general case, at a point where $f_i \neq 0$ and $g_{ij} \neq 0$.

Type	s_1-constraint	s_1'-constraint	$\frac{1}{Z_1}$ solution interval	Solution exists if
I	$1/Z_1 > s_1$	$1/Z_1 \geq s_1'$	$(\max(s_1, s_1', 0), \infty)$	always
II	$1/Z_1 > s_1$	$1/Z_1 \leq s_1'$	$(\max(s_1, 0), s_1')$	$s_1' \geq 0$ and $s_1 < s_1'$
III	$1/Z_1 < s_1$	$1/Z_1 \geq s_1'$	$(\max(s_1', 0), s_1)$	$s_1 > 0$ and $s_1' < s_1$
IV	$1/Z_1 < s_1$	$1/Z_1 \leq s_1'$	$(0, \min(s_1, s_1'))$	$s_1 > 0$ and $s_1' \geq 0$

If some of f_i, g_{ij} are zero at a point, we may obtain constraints that do not depend on Z_1, or equality constraints.

In the table above each image point is assigned to one of four categories (see Figure 4 for an example). Whether, for a given image point, there actually exists a value for $\frac{1}{Z_1}$ satisfying the constraints depends on whether the solution interval at that point is empty or not. Thus we classify all image points on the sphere into three categories, A, B, and C, depending on the kind of solution interval that exists for Z_1:(A) there exists no solution for Z_1; or there exists a solution, and the interval for Z_1 is (B) bounded, or (C) unbounded. In the latter two cases, we can also check whether the interval has a lower bound greater than 0.

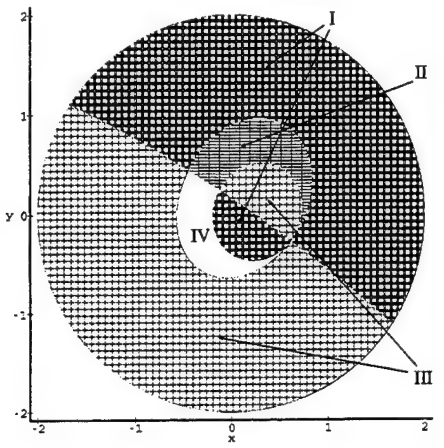

Figure 4: Classification of image points by s_1-constraint and s_1'-constraint.

The classification of a point into one of the categories (I–IV) depends on the signs of f_t, g_{21}, and g_{22}. The existence of a solution interval at a point also depends on the signs of f_ω and g_{12} at that point and also on the relative values of s_1 and s_1', i.e., on the sign of $s_1 - s_1'$.

Functions $f_i(\mathbf{r})$ and $g_{ij}(\mathbf{r})$ are polynomial functions of $\mathbf{r}$. To find out where they change sign, it is enough to find points where they are zero. The sign of $s_1 - s_1'$ is more complicated, since $s_1(\mathbf{r})$ and $s_1'(\mathbf{r})$ do not have to be continuous. However their discontinuities occur at points where $f_t(\mathbf{r}) = 0$ or $g_{21}(\mathbf{r}) = 0$. Thus $\mathrm{sgn}(s_1 - s_1')$ can change at those points and at points where $s_1 - s_1' = 0$. Using (5), we can write

$$s_1 - s_1' = -\frac{g_{12}}{f_t} - \frac{f_\omega}{g_{21}} = -\frac{1}{f_t\, g_{21}}(f_t\, f_\omega + g_{12}\, g_{21}) = -\frac{g_{11}\, g_{22}}{f_t\, g_{21}} \tag{17}$$

So we see that $\mathrm{sgn}(s_1 - s_1')$ can change only at points where at least one of f_i, g_{ij} is zero. At points where $g_{22} = 0$ we have the s_1-constraint $\frac{1}{Z_1} = s_1$ and the s_1'-constraint $\frac{1}{Z_1} = s_1'$. From equation (17) we obtain $s_1 = s_1'$; thus at these points the depth Z_1 is uniquely defined.

Let us consider the implicit curves $f_i(\mathbf{r}) = 0$ and $g_{ij}(\mathbf{r}) = 0$. In the general case, these equations describe two geodesics and four zero motion contours. Each of the curves divides the sphere into areas where the solution interval for Z_1 could be different (areas of class A, B, C). However, not every point on the curves separates different areas. Inside any of the areas, all the points have the same classification (for example an infinite solution interval for Z_1 with a positive lower bound). Figure 5 shows an example of this classification, although the derivation of how to actually obtain the areas where there does not exist a solution is

deferred to the next subsection.

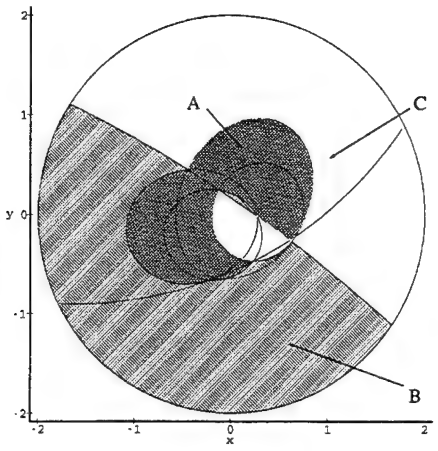

Figure 5: Classification of image points according to the solution interval. (The corresponding motion configuration is displayed in Figure 7.)

Up to this point we have been discussing only the constraints for Z_1. Similarly, from (11) and (12) we have at any point the s_2-constraint ($\frac{1}{Z_2} > s_2$, $\frac{1}{Z_2} = s_2$, or $\frac{1}{Z_2} < s_2$), and the s_2'-constraint ($\frac{1}{Z_2} \geq s_2'$, $\frac{1}{Z_2} = s_2'$, or $\frac{1}{Z_2} \leq s_2'$). We obtain the same curves dividing the sphere into areas such that inside any of the areas, the type of solution interval for Z_2 is the same.

Now we can summarize the results. The curves $f_i(\mathbf{r}) = 0$ and $g_{ij}(\mathbf{r}) = 0$ separate the sphere into a number of areas. Each of the areas is either contradictory (i.e., containing only contradictory points), or ambiguous (i.e., containing points where the two motion vectors can have the same direction). Two different rigid motions can produce ambiguous directions of flow if the image contains only points from ambiguous areas. There are also two scene surfaces constraining depth Z_1 and two surfaces constraining depth Z_2. If the depths do not satisfy the constraints, the two flows are not ambiguous.

3.4 Contradictory points

In this section we investigate conditions that must be satisfied when a point is contradictory. Since the type of solution for Z_1 and Z_2 depends on the signs of f_i and g_{ij}, we want to describe sign combinations that yield a contradiction. We investigate the general case, i.e., we assume $f_i \neq 0$, and $g_{ij} \neq 0$ and use the resulting constraints in Section 4. Special cases are treated separately in Section 5.

There are two simple conditions yielding contradiction for Z_1, one for the s_1-constraint and one for the s_1'-constraint. There is no solution for Z_1 if $\frac{1}{Z_1} < s_1$ and $s_1 \leq 0$. This happens under the following condition C_1:

$$\text{sgn}(f_t) = \text{sgn}(g_{12}) = -\text{sgn}(g_{22}) \tag{18}$$

which is derived from equation (9). Similarly, from (10) we get a contradiction if $\frac{1}{Z_1} \leq s_1'$ and $s_1' < 0$, i.e., under condition C_2:

$$\text{sgn}(f_\omega) = -\text{sgn}(g_{21}) = \text{sgn}(g_{22}) \tag{19}$$

We get similar conditions for Z_2. There is no solution for Z_2, if $\frac{1}{Z_2} < s_2$ and $s_2 \leq 0$, or if $\frac{1}{Z_2} \leq s_2'$ and $s_2' < 0$. This happens under conditions C_3 and C_4:

$$\text{sgn}(f_t) = -\text{sgn}(g_{21}) = \text{sgn}(g_{11}) \tag{20}$$

and

$$\text{sgn}(f_\omega) = \text{sgn}(g_{12}) = -\text{sgn}(g_{11}) \tag{21}$$

We call these four constraints (C_1–C_4) Contradictory Point conditions, or CP-conditions for short. Next we show that a point (where $f_i \neq 0$ and $g_{ij} \neq 0$) is contradictory if and only if at least one of the four conditions is satisfied.

Let us assume that conditions (18) and (19) are not satisfied at some point, but we have a contradiction for Z_1. Then the point must be of type II or III, since there is always a solution for points of type I, and a point of type IV is contradictory only if (18) or (19) holds.

For a point of type II, $\frac{1}{Z_1} \leq s_1'$, but (19) is not satisfied, so we have $s_1' \geq 0$. A contradiction is possible only if $s_1 \geq s_1'$. This happens when $\text{sgn}(g_{22}) = \text{sgn}(f_t)$, $\text{sgn}(g_{22}) \neq \text{sgn}(g_{21})$, $\text{sgn}(g_{12}) \neq \text{sgn}(f_t)$ and $\text{sgn}(f_\omega) = \text{sgn}(g_{21})$, i.e., when

$$\text{sgn}(g_{22}) = \text{sgn}(f_t) = -\text{sgn}(g_{21}) = -\text{sgn}(g_{21}) = -\text{sgn}(f_\omega)$$

and $s_1 - s_1' > 0$. Since $\text{sgn}(f_t) = -\text{sgn}(g_{21})$, from (17) we obtain

$$\text{sgn}(g_{11}) = \text{sgn}(g_{22}) = \text{sgn}(f_t) = -\text{sgn}(g_{21})$$

Thus in this case condition (20) holds.

We obtain the same result for points of type III. Since (18) is not satisfied, we have $s_1 > 0$. So a contradiction is possible only if $s_1 < s_1'$. This happens when

$$\text{sgn}(g_{22}) = -\text{sgn}(f_t) = \text{sgn}(g_{21}) = \text{sgn}(g_{21}) = \text{sgn}(f_\omega)$$

and $s_1 - s_1' < 0$. Since $\text{sgn}(f_t) = -\text{sgn}(g_{21})$, we obtain

$$\text{sgn}(g_{11}) = -\text{sgn}(g_{22}) = \text{sgn}(f_t) = -\text{sgn}(g_{21})$$

and again condition (20) holds.

Thus if there is no solution for Z_1, at least one of conditions (18), (19) and (20) must hold. Similarly if there is no solution for Z_2, at least one of conditions (18), (20) and (21) must hold.

By examination of all the possibilities, we can show that at any point, either none of the CP-conditions holds (and the point is ambiguous), or exactly two of the conditions hold (and the point is contradictory).

3.5 Antipodal pairs of points

In this section we investigate constraints for a point $\mathbf{r}$ and its antipodal point $-\mathbf{r}$ to be both ambiguous or to be both contradictory.

Again we describe a general case, i.e., assume $f_i \neq 0$ and $g_{ij} \neq 0$. We have $f_t(-\mathbf{r}) = -f_t(\mathbf{r})$, $f_\omega(-\mathbf{r}) = -f_\omega(\mathbf{r})$, but $g_{ij}(-\mathbf{r}) = g_{ij}(\mathbf{r})$. If $\text{sgn}(g_{12}(\mathbf{r})) \neq \text{sgn}(g_{22}(\mathbf{r}))$, then condition (18) holds either at $\mathbf{r}$, or at $-\mathbf{r}$. We get similar results for the remaining three CP-conditions. Thus both point $\mathbf{r}$ and point $-\mathbf{r}$ are ambiguous only if

$$\text{sgn}(g_{11}(\mathbf{r})) = \text{sgn}(g_{12}(\mathbf{r})) = \text{sgn}(g_{21}(\mathbf{r})) = \text{sgn}(g_{22}(\mathbf{r})) \tag{22}$$

Point $\mathbf{r}$ and point $-\mathbf{r}$ can also both be contradictory. As shown in Appendix F, this happens when

$$\text{sgn}(g_{11}(\mathbf{r})) = \text{sgn}(g_{22}(\mathbf{r})) = -\text{sgn}(g_{21}(\mathbf{r})) = -\text{sgn}(g_{22}(\mathbf{r})) \tag{23}$$

4 The Geometry of the Depth-Positivity Constraint

In the last section we found that if the CP-conditions hold at a point on the imaging surface, then one of the depth values has to be negative and thus the point is contradictory. In this section we investigate these constraints further; in particular we would like to know under what conditions two rigid motions cannot be distinguished if our imaging surface is a half sphere or an image plane, and we are interested in studying and visualizing the locations of areas where the CP-conditions are met.

Considering as imaging surface the whole sphere, two different rigid motions cannot produce flow of the same direction everywhere. As shown in Section 3.5, two antipodal points $\mathbf{r}$ and $-\mathbf{r}$ are ambiguous only if (22) holds. Thus for any point on curve $g_{ij} = 0$, since the sign of g_{ij} is positive on one side of the curve and negative on the other, there must exist a neighborhood either around $\mathbf{r}$ or around $-\mathbf{r}$ where there is a contradiction.

We are now ready, using the machinery already developed, to study uniqueness properties. As in the previous section, we assume that vectors $\mathbf{t}_1$, $\mathbf{t}_2$, $\boldsymbol{\omega}_1$, and $\boldsymbol{\omega}_2$ are of unit length.

4.1 Half sphere image: The general case

Let us assume that the image is a half of the sphere. Let us also assume that

$$(\boldsymbol{\omega}_1 \times \boldsymbol{\omega}_2) \cdot (\mathbf{t}_1 \times \mathbf{t}_2) \neq 0 \tag{24}$$

We show that under this condition the two rigid motions cannot produce motion fields with the same direction everywhere in the image.

Let us consider the projections of $\boldsymbol{\omega}_1$ and $\boldsymbol{\omega}_2$ on a geodesic n connecting $\mathbf{t}_1$ and $\mathbf{t}_2$. Projection onto the geodesic is well defined for all points $\mathbf{r}$ such that $\mathbf{r} \times (\mathbf{t}_1 \times \mathbf{t}_2) \neq 0$. Since we assume (24), the projections of both $\boldsymbol{\omega}_1$ and $\boldsymbol{\omega}_2$ are well defined. The proof is given in parts A and B.

A: Let us first assume that one of $\boldsymbol{\omega}_1$, $\boldsymbol{\omega}_2$ does not lie on geodesic n. Without loss of generality, let it be $\boldsymbol{\omega}_1$, i.e., let $[\mathbf{t}_1\, \mathbf{t}_2\, \boldsymbol{\omega}_1] \neq 0$.

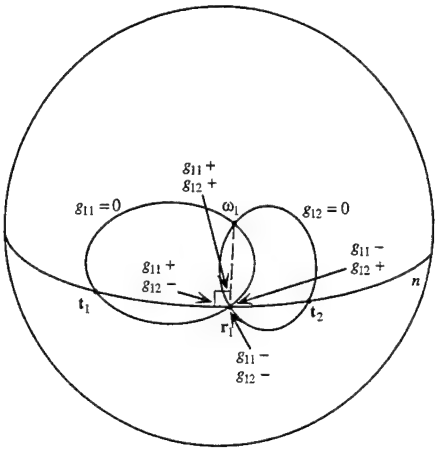

Figure 6: Possible sign combinations of g_{11} and g_{12} in the neighborhood of $\mathbf{r}_1$.

The projection of $\boldsymbol{\omega}_1$ onto n is

$$\mathbf{r}_1 = \pm(\mathbf{t}_1 \times \mathbf{t}_2) \times (\boldsymbol{\omega}_1 \times (\mathbf{t}_1 \times \mathbf{t}_2)) \tag{25}$$

where the sign is chosen so that $\mathbf{r}_1$ is in the image. Then

$$\begin{aligned} f_\omega(\mathbf{r}_1) &= \pm((\boldsymbol{\omega}_1 \times \boldsymbol{\omega}_2) \times (\mathbf{t}_1 \times \mathbf{t}_2)) \cdot (\boldsymbol{\omega}_1 \times (\mathbf{t}_1 \times \mathbf{t}_2)) \\ &= \mp[\mathbf{t}_1\, \mathbf{t}_2\, \boldsymbol{\omega}_1]((\boldsymbol{\omega}_1 \times \boldsymbol{\omega}_2) \cdot (\mathbf{t}_1 \times \mathbf{t}_2)) \qquad \neq \ 0 \end{aligned} \tag{26}$$

and $g_{11}(\mathbf{r}_1) = g_{12}(\mathbf{r}_1) = 0$. So the s_2'-constraint is $\text{sgn}(\frac{1}{Z_1}0) = \text{sgn}(\frac{1}{Z_2}0 + f_\omega)$ or $f_\omega = 0$. Clearly, this constraint cannot be satisfied, so $\mathbf{r}_1$ is a contradictory point.

We can also show that at least one of the areas around point $\mathbf{r}_1$ is contradictory. Point $\mathbf{r}_1$ lies on zero motion contours $g_{11}(\mathbf{r}) = 0$ and $g_{12}(\mathbf{r}) = 0$. If the two contours cross at this point (Appendix C shows that $g_{11}(\mathbf{r}) = 0$ and $g_{12}(\mathbf{r}) = 0$ at $\mathbf{r}_1$ cannot be tangent), we obtain four areas in the neighborhood of $\mathbf{r}_1$, and all four possible sign combinations of g_{11} and g_{12}. If we look at points close enough to $\mathbf{r}_1$ (so that f_ω does not change sign), then condition (21) is satisfied in one of the areas, and that area is contradictory. For an illustration see Figure 6.

B: Now we need to consider the situation where both $\boldsymbol{\omega}_1$ and $\boldsymbol{\omega}_2$ lie on geodesic n, i.e., $[\mathbf{t}_1\, \mathbf{t}_2\, \boldsymbol{\omega}_1] = [\mathbf{t}_1\, \mathbf{t}_2\, \boldsymbol{\omega}_2] = 0$. Let us consider point $\boldsymbol{\omega}_1$. We know $f_t(\boldsymbol{\omega}_1) = g_{11}(\boldsymbol{\omega}_1) = g_{12}(\boldsymbol{\omega}_1) = 0$. Also $g_{2i}(\boldsymbol{\omega}_1) = (\boldsymbol{\omega}_2 \times \boldsymbol{\omega}_1) \cdot (\mathbf{t}_i \times \boldsymbol{\omega}_1)$. Since both $\boldsymbol{\omega}_1$ and $\boldsymbol{\omega}_2$ lie on geodesic n, $(\boldsymbol{\omega}_2 \times \boldsymbol{\omega}_1)$ is parallel to $(\mathbf{t}_i \times \boldsymbol{\omega}_1)$. Thus $g_{2i}(\boldsymbol{\omega}_1)$ is zero only if $(\mathbf{t}_i \times \boldsymbol{\omega}_1)$ is zero. However, from (24) we have $(\mathbf{t}_1 \times \mathbf{t}_2) \neq 0$, so either g_{21} or g_{22} is non-zero at $\boldsymbol{\omega}_1$.

If $g_{21}(\boldsymbol{\omega}_1) \neq 0$, then condition (11) cannot be satisfied and $\boldsymbol{\omega}_1$ is a contradictory point. Again, it is not a singular point. The line tangent to g_{11} at $\boldsymbol{\omega}_1$ has direction $\boldsymbol{\omega}_1 \times \mathbf{t}_1$ (and $\boldsymbol{\omega}_1 \times \mathbf{t}_1 \neq 0$, since $g_{21}(\boldsymbol{\omega}_1) \neq 0$), so g_{11} is perpendicular to n at this point. Since f_t is identical to n, curves $g_{11} = 0$ and $f_t = 0$ create four areas around $\boldsymbol{\omega}_1$ with all possible sign combinations. Thus in one of the areas, condition (20) holds, and we obtain a contradictory area.

If $g_{22}(\boldsymbol{\omega}_1) \neq 0$, then condition (9) cannot be satisfied at $\boldsymbol{\omega}_1$. Again, at least one area around $\boldsymbol{\omega}_1$ is contradictory, since contour $g_{12} = 0$ is perpendicular to n at this point. This concludes the proof that if (24) is satisfied there exist contradictory areas on the half sphere. Section 4.2 discusses the case when (24) is not satisfied.

The rest of this section describes properties of the contradictory areas in order to provide a geometric intuition.

Just as we projected $\boldsymbol{\omega}_1$ on geodesic n connecting $\mathbf{t}_1$ and $\mathbf{t}_2$ to obtain $\mathbf{r}_1$, we project $\boldsymbol{\omega}_2$ on n to obtain $\mathbf{r}_2$, and we project $\mathbf{t}_1$ and $\mathbf{t}_2$ on geodesic l, connecting $\boldsymbol{\omega}_1$ and $\boldsymbol{\omega}_2$, to obtain $\mathbf{r}_3$ and $\mathbf{r}_4$ (see Figure 7). Point $\mathbf{r}_2$ is at the intersection of $f_t = 0$, $g_{21} = 0$, and $g_{22} = 0$; $\mathbf{r}_3$ is at the intersection of $f_\omega = 0$, $g_{11} = 0$, and $g_{21} = 0$; and $\mathbf{r}_4$ is at the intersection of $f_\omega = 0$, $g_{12} = 0$, and $g_{22} = 0$. By the same argumentation as before, at each of the points we can choose two of the contours $f_i = 0$ and $g_{ij} = 0$ passing through the point and we obtain four areas of different sign combinations in the corresponding terms f_i and g_{ij} around the point; it can be shown that one of these areas is contradictory because one of the CP-conditions is met.

The CP-conditions are constraints on the signs of the terms f_i and g_{ij}. Thus the boundaries of the contradictory areas are formed by the curves $f_i = 0$ and $g_{ij} = 0$. As we have shown the contradictory area and its boundaries must contain the points $\mathbf{r}_1$, $\mathbf{r}_2$, $\mathbf{r}_3$, and $\mathbf{r}_4$. For some motion configurations the boundaries also might contain $\mathbf{t}_1$, $\mathbf{t}_2$, $\boldsymbol{\omega}_1$, and $\boldsymbol{\omega}_2$. It can, however, be verified that no neighborhood around $\mathbf{t}_1$, $\mathbf{t}_2$, $\boldsymbol{\omega}_1$, and $\boldsymbol{\omega}_2$ needs to be contradictory. It can also be verified, by examining all the possibilities for the signs of terms f_i and g_{ij} in the CP-conditions, that points $\mathbf{t}_1$, $\mathbf{t}_2$, $\boldsymbol{\omega}_1$, and $\boldsymbol{\omega}_2$ cannot lie inside a contradictory area, since at least one of their neighboring areas is ambiguous. Figures 8 and 9 show the contradictory areas for both halves of the sphere for two different motion configurations.

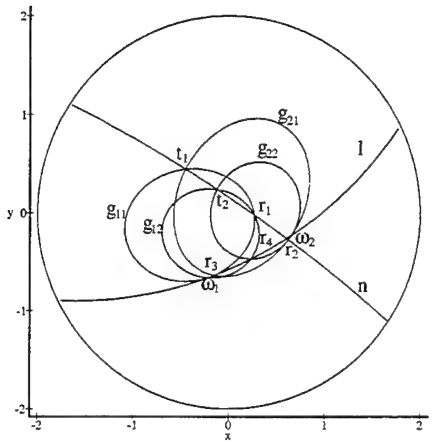

Figure 7: Separation of the sphere through curves $f_i = 0$ and $gij = 0$. Each of $\mathbf{t}_1$, $\mathbf{t}_2$, $\boldsymbol{\omega}_1$, $\boldsymbol{\omega}_2$, $\mathbf{r}_1$, $\mathbf{r}_2$, $\mathbf{r}_3$, and $\mathbf{r}_4$ lies at the intersection of three curves.

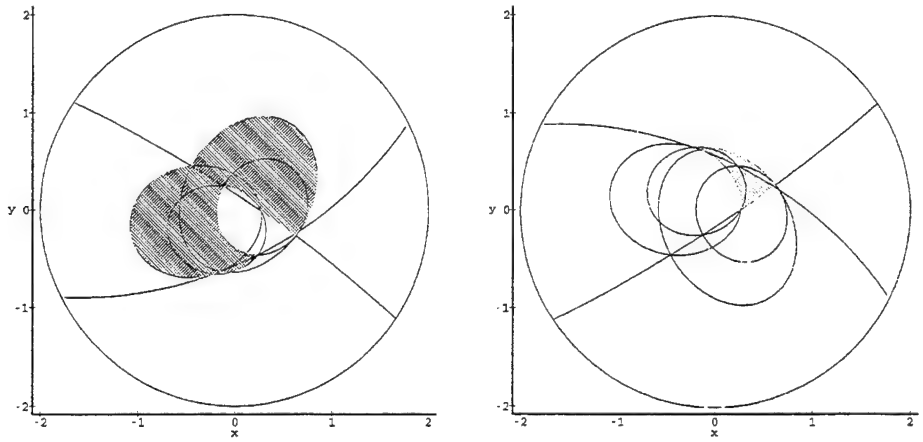

Figure 8: Contradictory areas for both halves of the sphere for the two motions shown in Figure 7.

Finally, let us consider the boundaries of the contradictory areas. As defined in Section 3, we allow the depths of the surfaces in view to take any value greater than zero (including infinity). Thus at any point $\mathbf{r}$ the motion vector $\dot{\mathbf{r}}$ could be in the direction of $v_{\mathrm{rot}}(\mathbf{r})$, but not in the direction of $v_{\mathrm{tr}}(\mathbf{r})$. This allows us to describe the depth values at possible boundaries of a contradictory area: At points on curve $f_\omega = 0$ both Z_1 and Z_2 can be infinite, thus boundary points on this curve are not elements of the contradictory area. Boundary points on all other curves ($f_t = 0$, or $g_{ij} = 0$) are contradictory, since one of the depths Z_1 and Z_2

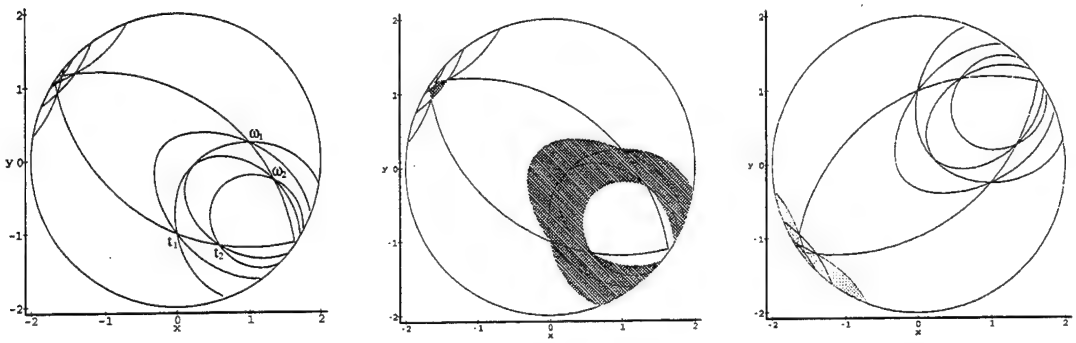

(a) (b) (c)

Figure 9: (a) Motion configuration. (b) and (c) Contradictory areas for both halves of the sphere.

would have to be zero.

4.2 Half sphere image: The case when $(\mathbf{t}_1 \times \mathbf{t}_2)$ is perpendicular to $(\boldsymbol{\omega}_1 \times \boldsymbol{\omega}_2)$

In this section it is shown that there could exist $(\mathbf{t}_1, \boldsymbol{\omega}_1)$ and $(\mathbf{t}_2, \boldsymbol{\omega}_2)$, with $(\mathbf{t}_1 \times \mathbf{t}_2)$ perpendicular to $(\boldsymbol{\omega}_1 \times \boldsymbol{\omega}_2)$, such that there exist no contradictory areas in one hemisphere.

First we investigate possible positions of points $\mathbf{t}_1$, $\mathbf{t}_2$, $\boldsymbol{\omega}_1$ and $\boldsymbol{\omega}_2$ on the hemisphere, bounded by equator q. Then we describe additional conditions on the orientation of vectors $\mathbf{t}_i$ and $\boldsymbol{\omega}_i$ with respect to the hemisphere.

As shown in Section 3.5, two antipodal points $\mathbf{r}$ and $-\mathbf{r}$ can be ambiguous only if (22) holds. Thus if the border of the area defined by (22) intersects q, there will be a contradiction in the image.

If curve $g_{ij} = 0$ intersects q at point $\mathbf{p}$, at least one of the areas around $\mathbf{p}$ does not satisfy condition (22). Unless $\mathbf{t}_1$, $\mathbf{t}_2$, $\boldsymbol{\omega}_1$ and $\boldsymbol{\omega}_2$ all are on the boundary of the hemisphere (and then the motions are not ambiguous), there is a contradictory area in the image (either around $\mathbf{p}$, or around $-\mathbf{p}$).

Let $\mathbf{n}_0$ be the normal to the plane of q. By intersecting the zero motion contour $g_{ij} = 0$ with the border q of the hemisphere (see Appendix D), we find that real solutions for the intersection point are obtained only if

$$l = [\mathbf{t}\boldsymbol{\omega}\mathbf{n}_0]^2 - 4(\boldsymbol{\omega} \cdot \mathbf{n}_0)(\mathbf{t} \cdot \mathbf{n}_0)(\boldsymbol{\omega} \cdot \mathbf{t}) \geq 0. \tag{27}$$

A half sphere contains for each of the translation vectors $\mathbf{t}_i$ and the rotation vectors $\boldsymbol{\omega}_i$, exactly one of the vectors $+\mathbf{t}_i$ or $-\mathbf{t}_i$ and $+\boldsymbol{\omega}_i$ or $-\boldsymbol{\omega}_i$. Let us refer to the vectors in the considered hemisphere as $\tilde{\mathbf{t}}_i$ and $\tilde{\boldsymbol{\omega}}_i$. From equation (27), taking into account that $(\tilde{\mathbf{t}}_i \cdot \mathbf{n}_0) \geq 0$ and $(\tilde{\boldsymbol{\omega}}_i \cdot \mathbf{n}_0) \geq 0$, we see that $l > 0$, either if for any $\tilde{\boldsymbol{\omega}}_i$, $\tilde{\mathbf{t}}_j$, $(\tilde{\boldsymbol{\omega}}_i \cdot \tilde{\mathbf{t}}_j) < 0$ (i.e., $\tilde{\boldsymbol{\omega}}_i$ and $\tilde{\mathbf{t}}_j$ form an angle greater than 90°), or $(\tilde{\boldsymbol{\omega}}_i \cdot \tilde{\mathbf{t}}_j) > 0$ and $\tilde{\boldsymbol{\omega}}_i$ and $\tilde{\mathbf{t}}_j$ are such that $[\mathbf{t}_j \boldsymbol{\omega}_i \mathbf{n}_0]^2 > 4(\boldsymbol{\omega}_i \cdot \mathbf{n}_0)(\mathbf{t}_j \cdot \mathbf{n}_0)(\boldsymbol{\omega}_i \cdot \mathbf{t}_j)$, which means that $\tilde{\boldsymbol{\omega}}_i$ and $\tilde{\mathbf{t}}_j$ must be close to the border.

When $f_t = 0$ is perpendicular to $f_\omega = 0$, the projections of $\boldsymbol{\omega}_1$ and $\boldsymbol{\omega}_2$ on $f_t = 0$ and the projections of $\mathbf{t}_1$ and $\mathbf{t}_2$ on $f_\omega = 0$ coincide in one point $\mathbf{r}_1$, i.e., $\mathbf{r}_1 = \mathbf{r}_2 = \mathbf{r}_3 = \mathbf{r}_4$. Point $\mathbf{r}_1$ lies at the intersection of all six curves $f_i = 0$ and $g_{ij} = 0$.

Any three curves $f_i = 0$, $g_{jj} = 0$ and $g_{kl} = 0$ (with $k \neq l$) intersect only in $\mathbf{r}_1$ and one of the points $\tilde{\mathbf{t}}_1$, $\tilde{\mathbf{t}}_2$, $\tilde{\boldsymbol{\omega}}_1$, or $\tilde{\boldsymbol{\omega}}_2$. Furthermore, since all the zero motion contours have to be closed curves on the hemisphere, we conclude that if there exists a contradictory area, it also has to be in a neighborhood of $\mathbf{r}_1$. It thus suffices to consider all possible sign combinations of terms f_i and g_{ij} around $\mathbf{r}_1$. It can be verified that, for a hemisphere to contain only ambiguous areas, the two translations have to have the same sign, that is $\mathrm{sgn}(\mathbf{t}_1 \cdot \mathbf{n}_0) = \mathrm{sgn}(\mathbf{t}_2 \cdot \mathbf{n}_0)$. Also the two rotations have to have the same sign, i.e., $\mathrm{sgn}(\boldsymbol{\omega}_1 \cdot \mathbf{n}_0) = \mathrm{sgn}(\boldsymbol{\omega}_2 \cdot \mathbf{n}_0)$. Furthermore, the relative positions of $\mathbf{t}_1$, $\mathbf{t}_2$, $\boldsymbol{\omega}_1$, and $\boldsymbol{\omega}_2$ have to be such that

$$\mathrm{sgn}(((\boldsymbol{\omega}_1 \times \boldsymbol{\omega}_2) \times (\mathbf{t}_1 \times \mathbf{t}_2)) \cdot \mathbf{n}_0) = \mathrm{sgn}(\mathbf{t}_1 \cdot \mathbf{n}_0)\,\mathrm{sgn}(\boldsymbol{\omega}_1 \cdot \mathbf{n}_0)$$

Intuitively this means, when rotating $f_\omega = 0$ in the orientation given by the rotations in order to make $f_\omega = 0$ and $f_t = 0$ parallel, then the order of points $\mathbf{t}_1$ and $\mathbf{t}_2$ on $f_t = 0$ is opposite to the order of points $\tilde{\boldsymbol{\omega}}_1$ and $\tilde{\boldsymbol{\omega}}_2$ on $f_\omega = 0$ (moving along the same direction along $f_\omega = 0$ and $f_t = 0$), if $\mathrm{sgn}(\mathbf{t}_1 \cdot \mathbf{n}_0) = 1$. Otherwise, if $\mathrm{sgn}(\mathbf{t}_1 \cdot \mathbf{n}_0) = -1$, the order of points $-\mathbf{t}_1$ and $-\mathbf{t}_2$ on $f_t = 0$ must be the same as the order of points $\tilde{\boldsymbol{\omega}}_1$ and $\tilde{\boldsymbol{\omega}}_2$ on $f_\omega = 0$.

In summary, we have shown that two rigid motions could be ambiguous on one hemisphere, if $(\mathbf{t}_1 \times \mathbf{t}_2)$ is perpendicular to $(\boldsymbol{\omega}_1 \times \boldsymbol{\omega}_2)$, but only if certain sign and certain distance conditions on $\mathbf{t}_1$, $\mathbf{t}_2$, $\boldsymbol{\omega}_1$ and $\boldsymbol{\omega}_2$ are met. In addition, as shown in Section 3, the two surfaces in view are constrained by a second and a third order surface (as shown in equations (15) and (16)). Figure 10 gives an example of such a configuration.

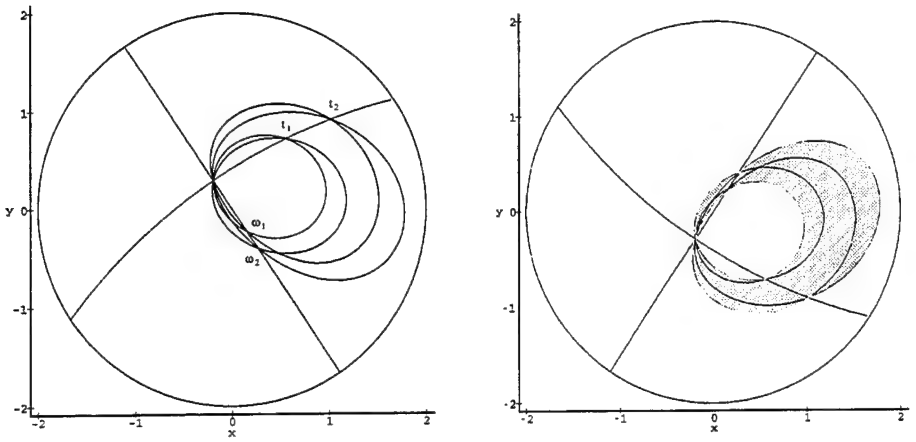

(a) (b)

Figure 10: Both halves of the sphere showing two rigid motions for which there do not exist contradictory areas in one hemisphere. (a) Hemisphere containing only ambiguous areas. (b) Contradictory areas for the other hemisphere.

In the next section we discuss the special cases and show that they do not allow for ambiguity. Thus the case of $(\mathbf{t}_1 \times \mathbf{t}_2)$ being perpendicular to $(\boldsymbol{\omega}_1 \times \boldsymbol{\omega}_2)$ is the only case where two motions can produce the same direction of the motion field on a hemisphere. An analysis concerned with ambiguities due to more than two rigid motions is given in Appendix A.

5 Special Cases

In previous sections, we assumed that $\mathbf{t}_1 \times \mathbf{t}_2 \neq 0$ and $\boldsymbol{\omega}_1 \times \boldsymbol{\omega}_2 \neq 0$. Here we show that if these conditions do not hold, then the two motions are not ambiguous.

In Section 3 we assumed all four vectors $\mathbf{t}_1$, $\mathbf{t}_2$, $\boldsymbol{\omega}_1$, and $\boldsymbol{\omega}_2$ to be of unit length. Here the four vectors can also be zero. Thus we have two different motions (i.e. $\mathbf{t}_1 \neq \mathbf{t}_2$, or $\boldsymbol{\omega}_1 \neq \boldsymbol{\omega}_2$), such that $\mathbf{t}_1 \times \mathbf{t}_2 = 0$ or/and $\boldsymbol{\omega}_1 \times \boldsymbol{\omega}_2 = 0$.

To cover all possible cases we are required to make a minor assumption about the depth Z_1 and Z_2 for the case where $\boldsymbol{\omega}_1 = \boldsymbol{\omega}_2$.

Let $\boldsymbol{\omega}_1 = \boldsymbol{\omega}_2$. Then we have $\mathbf{t}_1 \neq \mathbf{t}_2$, and $f_\omega = 0$ everywhere. From (10) we obtain the constraint $\text{sgn}(\frac{1}{Z_1} g_{21}) = \text{sgn}(\frac{1}{Z_2} g_{22})$. So at points where g_{21} and g_{22} have different signs, the only possible solution is $\frac{1}{Z_1} = \frac{1}{Z_2} = 0$. Infinite values for both depths in these areas would

result in pure rotational flow fields in these areas and thus in an ambiguity. The same kind of ambiguity would occur if we considered the full flow. Therefore it seems reasonable to assume that at least at one point in the areas where $g_{11}g_{22} < 0$, depths Z_1 and Z_2 are not both infinite. Under this assumption there does not exist ambiguity for the case of $\boldsymbol{\omega}_1 = \boldsymbol{\omega}_2$. In the following we thus assume $\boldsymbol{\omega}_1 \neq \boldsymbol{\omega}_2$.

Next we provide a lemma that will be of use in the following proofs concerned with special cases as well as in the proof for full flow in Section 6.

Lemma: Let $\boldsymbol{\omega}_i \neq 0$, $\mathbf{t}_j \neq 0$. As in the previous section, let the image be a half sphere with equator q, let $\mathbf{n}_0$ be a unit vector normal to the plane of q. Then equation

$$\operatorname{sgn}(\frac{1}{Z} f_t) = \sigma \operatorname{sgn}(g_{ij}) \tag{28}$$

where $\sigma = \pm 1$, can be satisfied everywhere in the image only if $\mathbf{t}_j \times \mathbf{n}_0 = 0$ and $\boldsymbol{\omega}_i \cdot \mathbf{t}_j = 0$.

Proof: Since $\boldsymbol{\omega}_i$ and $\mathbf{t}_j$ are non-zero, there are points in the image where $g_{ij} \neq 0$. Thus $\mathbf{t}_1 \times \mathbf{t}_2$ must be non-zero and geodesic n connecting $\mathbf{t}_1$ and $\mathbf{t}_2$ is well defined. Equation (28) can be satisfied only if the zero motion contour is degenerate, i.e., $\boldsymbol{\omega}_i \cdot \mathbf{t}_j = 0$ (as in Figure 14b). Then the contour consists of two great circles. One of the circles must be identical to the geodesic n, and the other circle must be identical to q, the border of the image. This is possible only if $\mathbf{t}_j \times \mathbf{n}_0 = 0$ (see Figure 11). □

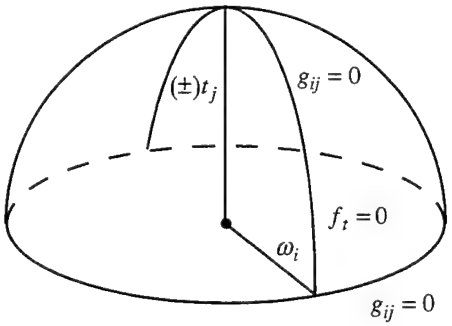

Figure 11: If $\operatorname{sgn}(\frac{1}{Z} f_t) = \sigma \operatorname{sgn}(g_{ij})$ everywhere, the zero motion contour $g_{ij} = 0$ consists of two great circles, one identical to the border of the hemisphere, the other identical to $f_t = 0$.

We now consider two special cases in parts A and B.

A: Let us assume that all $\mathbf{t}_i$ and $\boldsymbol{\omega}_i$ are non-zero.

If $\mathbf{t}_1 \times \mathbf{t}_2 = 0$, then f_t is zero everywhere. Thus from condition (9) we obtain $\text{sgn}(g_{12}) = \text{sgn}(g_{22})$. Since all four vectors are non-zero, this is possible only if $\boldsymbol{\omega}_1 \times \boldsymbol{\omega}_2 = 0$.

So we only need to consider the case $\boldsymbol{\omega}_1 \times \boldsymbol{\omega}_2 = 0$, and since we also assume $\boldsymbol{\omega}_1 \neq \boldsymbol{\omega}_2$, we have $\boldsymbol{\omega}_2 = -\boldsymbol{\omega}_1$. Then at any point in the image, $g_{2j}(\mathbf{r}) = -g_{1j}(\mathbf{r})$. Thus (9) can be satisfied only if $\text{sgn}(\frac{1}{Z_1} f_t) = \text{sgn}(g_{22})$. According to the lemma, this is possible only if $\mathbf{t}_2 \times \mathbf{n}_0 = 0$.

Similarly (11) can be satisfied only if $\text{sgn}(\frac{1}{Z_2} f_t) = \text{sgn}(g_{21})$. So from the lemma we obtain $\mathbf{t}_1 \times \mathbf{n}_0 = 0$. Therefore we have $\mathbf{t}_1 \times \mathbf{t}_2 = 0$, function f_t is zero everywhere, and the motions are contradictory.

B: If one of the motion parameters is zero, we obtain either a pure translational or a pure rotational flow field. By considering all the possible cases, it can be verified that the two motions are not ambiguous. Here we just consider one of the more difficult cases.

Let $\boldsymbol{\omega}_1 = 0$, $\boldsymbol{\omega}_2 \neq 0$, $\mathbf{t}_1 \neq 0$, and $\mathbf{t}_2 \neq 0$. Then at any point, $g_{11} = g_{12} = f_\omega = 0$. So from (9) we obtain $\text{sgn}(\frac{1}{Z_1} f_t) = \text{sgn}(g_{22})$, from (11) we have $0 = \text{sgn}(-\frac{1}{Z_2} f_t + g_{21})$, or $\text{sgn}(\frac{1}{Z_2} f_t) = \text{sgn}(g_{21})$. From the lemma, this is possible only if $\mathbf{t}_2 \times \mathbf{n}_0 = 0$ and $\mathbf{t}_1 \times \mathbf{n}_0 = 0$; thus again we obtain $\mathbf{t}_1 \times \mathbf{t}_2 = 0$ and the motions are contradictory.

If two of the motions are zero, that is if either $\mathbf{t}_1 = \mathbf{t}_2 = 0$ or $\mathbf{t}_1 = \boldsymbol{\omega}_2 = 0$ (or equivalently $\mathbf{t}_2 = \boldsymbol{\omega}_1 = 0$) we obtain either two rotational, or one translational and one rotational field, which obviously cannot have the same direction.

6 Ambiguities of the Full Flow

Next we investigate the question whether there can be any ambiguities at all if we consider the complete flow. Horn has shown in [6] that two motions can produce ambiguous flow fields only if the observed surfaces are certain hyperboloids of one sheet. We show that if we also consider the depth positivity constraint and if the image is a half of the sphere, then any two different motions can be distinguished.

Let the image be a hemisphere bounded by equator q. Let $\mathbf{n}_0$ be a unit vector normal to the plane of q. As in [6], let us assume that a motion $(\mathbf{t}_1, \boldsymbol{\omega}_1)$ along with a depth map Z_1,

and a motion $(\mathbf{t}_2, \boldsymbol{\omega}_2)$ along with a depth map Z_2, yield the same flow field. At each point we obtain a vector equation

$$-\frac{1}{Z_1}(\mathbf{r} \times (\mathbf{t}_1 \times \mathbf{r})) - \boldsymbol{\omega}_1 \times \mathbf{r} = -\frac{1}{Z_2}(\mathbf{r} \times (\mathbf{t}_2 \times \mathbf{r})) - \boldsymbol{\omega}_2 \times \mathbf{r} \tag{29}$$

Projecting on directions $\mathbf{t}_1 \times \mathbf{r}$ and $\mathbf{t}_2 \times \mathbf{r}$, we obtain equations for the two critical surfaces

$$\frac{1}{Z_1}[\mathbf{t}_1\mathbf{t}_2\mathbf{r}] + (\boldsymbol{\delta\omega} \times \mathbf{r}) \cdot (\mathbf{t}_2 \times \mathbf{r}) = 0 \tag{30}$$

$$\frac{1}{Z_2}[\mathbf{t}_1\mathbf{t}_2\mathbf{r}] + (\boldsymbol{\delta\omega} \times \mathbf{r}) \cdot (\mathbf{t}_1 \times \mathbf{r}) = 0 \tag{31}$$

where $\boldsymbol{\delta\omega} = \boldsymbol{\omega}_2 - \boldsymbol{\omega}_1$.

If $\mathbf{t}_1 \neq 0$, $\mathbf{t}_2 \neq 0$, and $\boldsymbol{\delta\omega} \neq 0$, then according to the lemma in the previous section, these equations can be satisfied everywhere in the image only if $\boldsymbol{\delta\omega} \cdot \mathbf{t}_1 = 0$, $\mathbf{t}_1 \times \mathbf{n}_0 = 0$, $\boldsymbol{\delta\omega} \cdot \mathbf{t}_2 = 0$, and $\mathbf{t}_2 \times \mathbf{n}_0 = 0$. Thus we we obtain $\mathbf{t}_1 \times \mathbf{t}_2 = 0$. (This case corresponds to Section 4.5 in [6], that is, to the case when both critical surfaces consist of intersecting planes.) Therefore we are left only with special cases: Ambiguity can occur only if $\mathbf{t}_1 \times \mathbf{t}_2 = 0$, or $\boldsymbol{\delta\omega} = 0$.

If $\mathbf{t}_1 \times \mathbf{t}_2 = 0$ and $\boldsymbol{\delta\omega} \neq 0$, from constraint (30) we get for any $\mathbf{r}$

$$(\boldsymbol{\delta\omega} \times \mathbf{r}) \cdot (\mathbf{t}_2 \times \mathbf{r}) = 0 \tag{32}$$

Since $\boldsymbol{\delta\omega} \neq 0$, $\mathbf{t}_2$ must be zero. Similarly from constraint (31) we get $\mathbf{t}_1 = 0$. Thus we have a pair of rigid motions with different rotations and zero translations. Clearly these two motions are not ambiguous.

There is one special case left, $\boldsymbol{\delta\omega} = 0$. At each point we get a vector equation

$$-\frac{1}{Z_1}(\mathbf{r} \times (\mathbf{t}_1 \times \mathbf{r})) = -\frac{1}{Z_2}(\mathbf{r} \times (\mathbf{t}_2 \times \mathbf{r})) \tag{33}$$

Since we have two different motions and $\boldsymbol{\delta\omega} = 0$, we know $\mathbf{t}_1 \neq \mathbf{t}_2$. So the equation can be satisfied only when $\frac{1}{Z_1} = \frac{1}{Z_2} = 0$ for all points not lying on geodesic n passing through $\mathbf{t}_1$ and $\mathbf{t}_2$. If we do not allow infinite depth, the motions are not ambiguous.

7 Conclusions

In this paper we have analyzed the amount of information inherent in the directions of rigid flow fields. We have shown that in almost all cases there is enough information to determine

up to a multiplicative constant both the 3D-rotational and 3D-translational motion from a hemispherical image. Ambiguities can result only if the surfaces in view satisfy certain inequality and equality constraints. Furthermore, for two 3D motions to be compatible the two translation vectors must lie on a geodesic perpendicular to the geodesic through the two rotation vectors. With this analysis we have also shown that visual motion analysis does not necessarily require the intermediate computation of optical flow or exact correspondence. Instead, many dynamic vision problems might be solved with the use of more qualitative flow estimates if appropriate global constraints are found.

Appendix

Appendix A Ambiguity due to more than two motions

In this appendix we investigate whether three or more different rigid motions and their corresponding surfaces could possibly produce the same direction of the motion field on a hemisphere. We present proofs contradicting the ambiguity of almost all combinations of three rigid motions.

Let us consider any three different rigid motions $(\mathbf{t}_1, \boldsymbol{\omega}_1)$, $(\mathbf{t}_2, \boldsymbol{\omega}_2)$, and $(\mathbf{t}_3, \boldsymbol{\omega}_3)$, such that any two of the directional motion fields produced are the same, i.e. $(\mathbf{t}_i \times \mathbf{t}_j) \cdot (\boldsymbol{\omega}_i \times \boldsymbol{\omega}_j) = 0$ for $i = 1, \ldots, 3$, $j = 1, \ldots, 3$ with $i \neq j$. In the following proofs it will be shown that in general there exist areas in the image where the corresponding depth Z_3 cannot at the same time allow motions $(\mathbf{t}_1, \boldsymbol{\omega}_1)$ and $(\mathbf{t}_3, \boldsymbol{\omega}_3)$ and motions $(\mathbf{t}_2, \boldsymbol{\omega}_2)$ and $(\mathbf{t}_3, \boldsymbol{\omega}_3)$ to produce the same directional flow.

Let us consider the intersections of the zero motion contours $g_{ii} = 0$. In the sequel we consider separately in part A the general case where two of the zero motion contours intersect in at least two points, and in part B the case where any two zero motion contours are tangent to each other. (Appendix E describes the conditions on the motion parameters for two zero motion contours to be tangential.)

A: Let us assume that two of the zero motion contours are not tangential; let these be $g_{11} = 0$ and $g_{22} = 0$. Let $\mathbf{r}_{12}$ be the intersection point where $(\mathbf{t}_1 \times \mathbf{t}_2) \cdot \mathbf{r}_{12} = 0$ and

$(\omega_1 \times \omega_2) \cdot \mathbf{r}_{12} = 0$, and thus $v_{\mathrm{tr}_1}(\mathbf{r}_{12})$, $v_{\mathrm{tr}_2}(\mathbf{r}_{12})$, $v_{\mathrm{rot}_1}(\mathbf{r}_{12})$, $v_{\mathrm{rot}_2}(\mathbf{r}_{12})$ are parallel. Let $\mathbf{p}_{12}$ be another intersection point where g_{11} and g_{22} cross. Vectors $v_{\mathrm{rot}_1}(\mathbf{p}_{12})$ and $v_{\mathrm{rot}_2}(\mathbf{p}_{12})$ are not parallel, and $v_{\mathrm{tr}_1}(\mathbf{p}_{12}) = -\lambda_1 v_{\mathrm{rot}_1}(\mathbf{p}_{12})$ and $v_{\mathrm{tr}_2}(\mathbf{p}_{12}) = -\lambda_2 v_{\mathrm{rot}_2}(\mathbf{p}_{12})$ for some positive λ_1 and λ_2 (if λ_1 or λ_2 were negative, point $\mathbf{p}_{12}$ would be contradictory). Unless $g_{33}(\mathbf{p}_{12}) = 0$, we have $v_{\mathrm{tr}_3}(\mathbf{p}_{12}) \times v_{\mathrm{rot}_3}(\mathbf{p}_{12}) \neq 0$. Figure 12a shows a possible configuration of the motion vectors at $\mathbf{p}_{12}$.

We next consider the directions of $v_{\mathrm{rot}_i}(\mathbf{r})$ and $v_{\mathrm{tr}_i}(\mathbf{r})$ for points $\mathbf{r}$ in the neighborhood of $\mathbf{p}_{12}$. Let $\mathbf{n}_0$ be a unit vector in the direction $v_{\mathrm{tr}_3}(\mathbf{p}_{11}) \times v_{\mathrm{rot}_3}(\mathbf{p}_{12})$. For $i = 1..2$ the sign of $(v_{\mathrm{tr}_i}(\mathbf{r}) \times v_{\mathrm{rot}_i}(\mathbf{r})) \cdot \mathbf{n}_0$ changes from inside $g_{ii} = 0$ to outside $g_{ii} = 0$ (that is, for example, the angle between $v_{\mathrm{tr}_1}(\mathbf{r})$ and $v_{\mathrm{rot}_1}(\mathbf{r})$ is greater than 180° inside $g_{11} = 0$ and is smaller than 180° outside $g_{11} = 0$, or vice versa). The sign of $(v_{\mathrm{tr}_3}(\mathbf{r}) \times v_{\mathrm{rot}_3}(\mathbf{r})) \cdot \mathbf{n}_0$ is the same in a sufficiently small neighborhood around $\mathbf{p}_{12}$. Since $g_{11} = 0$ and $g_{22} = 0$ cross at $\mathbf{p}_{12}$ there are four neighborhoods around $\mathbf{p}_{12}$ with all four possible sign combinations of $(v_{\mathrm{tr}_1} \times v_{\mathrm{rot}_1}) \cdot \mathbf{n}_0$ and $(v_{\mathrm{tr}_2} \times v_{\mathrm{rot}_2}) \cdot \mathbf{n}_0$. Thus for points $\mathbf{r}$ in one of the neighborhoods, in order for $v_{\mathrm{tr}_1}(\mathbf{r}) + v_{\mathrm{rot}_1}(\mathbf{r})$ to have the same direction as $v_{\mathrm{tr}_3}(\mathbf{r}) + v_{\mathrm{rot}_3}(\mathbf{r})$, Z_3 must lie in an interval $[a, b]$, and for $v_{\mathrm{tr}_2}(\mathbf{r}) + v_{\mathrm{rot}_2}(\mathbf{r})$ to have the same direction as $v_{\mathrm{tr}_3}(\mathbf{r}) + v_{\mathrm{rot}_3}(\mathbf{r})$, Z_3 must lie in an interval $[c, d]$, where the intersection of $[a, b]$ and $[c, d]$ is empty. Therefore the three motions cannot give rise to the same direction at $\mathbf{r}$. For an example see Figure 12b.

B: We next consider the case where all three zero motion contours are tangent to each other. For the case where not all three are tangential at the same point, using arguments similar to those used before, we prove that there cannot be an ambiguity.

For at least two of the zero motion contours, say $g_{11} = 0$ and $g_{22} = 0$, we have that at the intersection point $\mathbf{r}_{12}$ the two curvature vectors $\kappa_{g_{11}}(\mathbf{r}_{12})$ of $g_{11} = 0$ and $\kappa_{g_{22}}(\mathbf{r}_{12})$ of $g_{22} = 0$ have opposite sign. Also, the translational and rotational components are such that $v_{\mathrm{tr}_1} = \lambda_1 v_{\mathrm{rot}_2} = -\lambda_2 v_{\mathrm{tr}_2} = -\lambda_3 v_{\mathrm{rot}_1}$ for $\lambda_1, \lambda_2, \lambda_3 \geq 0$ (see Figure 13a and b for an illustration). Let $\mathbf{n}_0$ be a unit vector in the direction $v_{\mathrm{tr}_3}(\mathbf{r}_{12}) \times v_{\mathrm{rot}_3}(\mathbf{r}_{12})$. At points $\mathbf{r}$ in the neighborhood of $\mathbf{r}_{12}$ we obtain three of the four possible sign combinations for the signs of $(v_{\mathrm{rot}_1}(\mathbf{r}) \times v_{\mathrm{tr}_1}(\mathbf{r})) \cdot \mathbf{n}_0$ and $(v_{\mathrm{tr}_2}(\mathbf{r}) \times v_{\mathrm{rot}_2}(\mathbf{r})) \cdot \mathbf{n}_0$. In both areas outside $g_{11} = 0$ and outside $g_{22} = 0$ we have $((v_{\mathrm{rot}_1}(\mathbf{r}) \times v_{\mathrm{tr}_1}(\mathbf{r})) \cdot \mathbf{n}_0)(v_{\mathrm{tr}_2}(\mathbf{r}) \times v_{\mathrm{rot}_2}(\mathbf{r})) \cdot \mathbf{n}_0) < 0$, but in one of

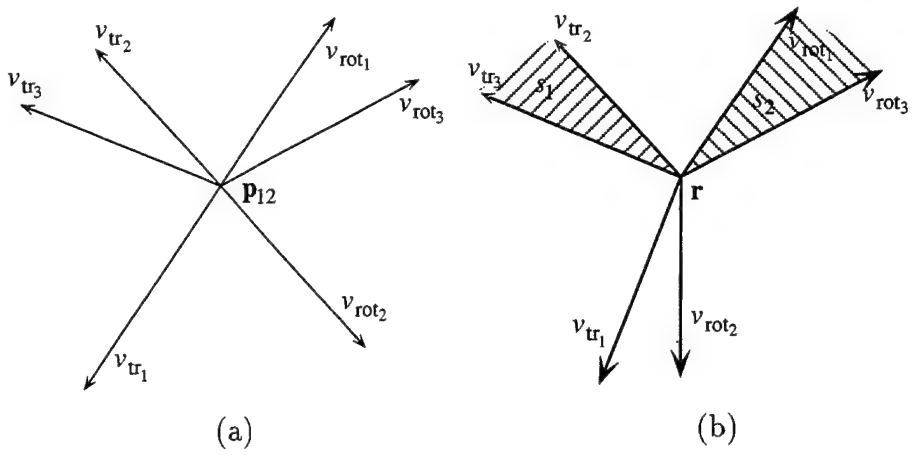

Figure 12: (a) Possible motion configuration at point $\mathbf{p}_{12}$. (b) There must exist a neighborhood around $\mathbf{p}_{12}$ with points $\mathbf{r}$, such that for $\mathbf{n}_0 = v_{tr_3}(\mathbf{p}_{12}) \times v_{rot_3}(\mathbf{p}_{12}) / |v_{tr_3}(\mathbf{p}_{12}) \times v_{rot_3}(\mathbf{p}_{12})|$, $(v_{rot_1} \times v_{tr_1}) \cdot \mathbf{n}_0 > 0$ and $(v_{tr_2} \times v_{rot_2}) \cdot \mathbf{n}_0 < 0$. In order for $\mathbf{u}_3 = v_{tr_1}(\mathbf{r}) + v_{rot_1}(\mathbf{r}) = \lambda_1(v_{tr_3}(\mathbf{r}) + v_{rot_3}(\mathbf{r}))$, $\mathbf{u}_3$ has to be in the sector S_1 and Z_3 has to take values in the interval $(0, b]$. In order for $\mathbf{u}_3 = v_{tr_2}(\mathbf{r}) + v_{rot_2}(\mathbf{r}) = \lambda_2(v_{tr_3}(\mathbf{r}) + v_{rot_3}(\mathbf{r}))$, $\mathbf{u}_3$ has to be in the sector S_2 and Z_3 has to take values in the interval $[c, \infty]$ with $b < c$.

the areas $(v_{tr_2}(\mathbf{r}) \times v_{rot_1}(\mathbf{r})) \cdot \mathbf{n}_0 > 0$ and in the other $(v_{tr_2}(\mathbf{r}) \times v_{rot_1}(\mathbf{r})) \cdot \mathbf{n}_0 < 0$. Since $(v_{tr_3}(\mathbf{r}) \times v_{rot_3}(\mathbf{r})) \cdot \mathbf{n}_0$ doesn't change sign in the neighborhood of $\mathbf{r}_{12}$, in one of the two areas the depth Z_3 of the third surface cannot be compatible with both the first and the second motion (see Figure 13c).

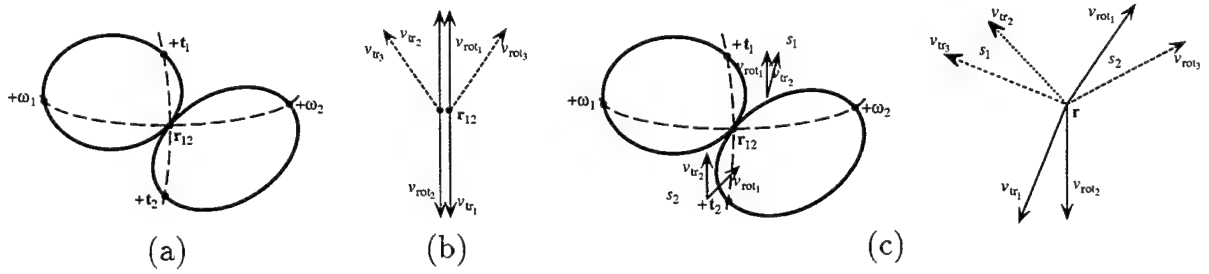

Figure 13: (a) Intersection of zero motion contours $g_{11} = 0$ and $g_{22} = 0$ at point $\mathbf{r}_{12}$ with $\kappa_{g_{11}}(\mathbf{r}_{12})\kappa_{g_{22}}(\mathbf{r}_{12}) < 0$. (b) Possible motion configuration at point $\mathbf{r}_{12}$. (c) At point $\mathbf{r}$ in one of the areas outside $g_{11} = 0$ and outside $g_{22} = 0$ (here S_2) the depth of Z_3 cannot be compatible with both $(v_{tr_1}(\mathbf{r}), v_{rot_1}(\mathbf{r}))$ and $(v_{tr_2}(\mathbf{r}), v_{rot_2}(\mathbf{r}))$.

Thus, in summary we have shown that more than two different rigid motions can hardly ever give rise to the same direction of flow at every point on a hemisphere. The only possible

configurations of motions that may be contradictory, provided the surfaces in view satisfy the constraints described in Section 3, are:

a: three or more motions such that the corresponding zero motion contours $g_{ii} = 0$ intersect in the same point $\mathbf{p}_{ij}$, with $v_{\mathrm{tr}_i}(\mathbf{p}_{ij}) \times v_{\mathrm{tr}_j}(\mathbf{p}_{ij}) \neq 0$ for $i \neq j$.

b: three or more motions, such that all corresponding zero motion contours $g_{ii} = 0$ are tangential at the same point $\mathbf{r}_{12}$, which as described in Appendix E, can occur only if $\frac{\tan \angle(\mathbf{t}_i, \mathbf{r}_{12})}{\tan \angle(\boldsymbol{\omega}_i, \mathbf{r}_{12})} = C$ for some constant C.

Appendix B Zero motion contours

Let us consider the following question: What is the locus of points where the flow due to the given rigid motion can possibly be zero? As in [4] we can show that such points are constrained to lie on a second order curve on the sphere.

The flow at point $\mathbf{r}$ can be zero only if the rotational and translational components at $\mathbf{r}$ are parallel to each other. Let $\mathbf{t}$ and $\boldsymbol{\omega}$ be translational and rotational velocity of the observer. Then the flow at point $\mathbf{r}$ can be zero only if

$$(\mathbf{r} \times (\mathbf{t} \times \mathbf{r})) \times (\boldsymbol{\omega} \times \mathbf{r}) = 0 \tag{34}$$

By simple vector manipulation, from (34) we obtain

$$((\boldsymbol{\omega} \times \mathbf{r}) \cdot (\mathbf{t} \times \mathbf{r}))\mathbf{r} = 0 \tag{35}$$

Since $\mathbf{r} \neq 0$, the flow at point $\mathbf{r}$ can be zero only if

$$\begin{aligned} &(\boldsymbol{\omega} \times \mathbf{r}) \cdot (\mathbf{t} \times \mathbf{r}) = 0 \\ \text{or} \quad &\boldsymbol{\omega} \cdot \mathbf{t} - (\boldsymbol{\omega} \cdot \mathbf{r})(\mathbf{t} \cdot \mathbf{r}) = 0 \end{aligned} \tag{36}$$

Equation (36) describes a second order curve on the sphere, which we will call the zero motion contour of the rigid motion $(\mathbf{t}, \boldsymbol{\omega})$. The zero-motion contour consists of two closed curves on the sphere. As shown in Figure 14, if $(\boldsymbol{\omega} \cdot \mathbf{t}) > 0$, one of the curves contains $\mathbf{t_0} = \frac{\mathbf{t}}{|\mathbf{t}|}$ and $\boldsymbol{\omega}_0 = \frac{\boldsymbol{\omega}}{|\boldsymbol{\omega}|}$ and one contains $-\mathbf{t_0}$ and $-\boldsymbol{\omega}_0$; if $(\boldsymbol{\omega} \cdot \mathbf{t}) = 0$ the two curves become great circles, one orthogonal to $\mathbf{t}$, the other orthogonal to $\boldsymbol{\omega}$; if $(\boldsymbol{\omega} \cdot \mathbf{t}) < 0$ one of the two curves passes through $\mathbf{t}_0$ and $-\boldsymbol{\omega}_0$ and the other through $-\mathbf{t}_0$ and $\boldsymbol{\omega}_0$.

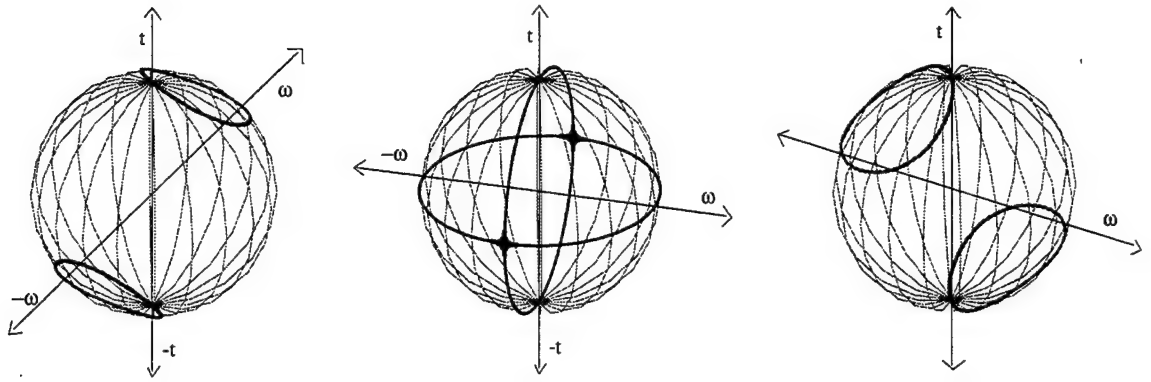

Figure 14: The zero motion contour (the locus of points $\mathbf{r}$ where $\dot{\mathbf{r}}$ could be zero) consists of two closed curves on the sphere. Three possible configurations are (a) $(\boldsymbol{\omega} \cdot \mathbf{t}) > 0$, (b) $(\boldsymbol{\omega} \cdot \mathbf{t}) = 0$, and (c) $(\boldsymbol{\omega} \cdot \mathbf{t}) < 0$.

Appendix C Zero motion contours are not tangent

To show that zero motion contours g_{11} and g_{12} are not tangent at $\mathbf{r}_1$ (see Section 4.1, part A), let us compute tangent lines to the contours at $\mathbf{r}_1$. Let the direction of the line tangent to g_{11} at $\mathbf{r}_1$ be $\mathbf{u}_1$. The line lies in the plane tangent to the sphere, so

$$\mathbf{u}_1 \cdot \mathbf{r}_1 = 0 \tag{37}$$

Directional derivative of g_{11} along $\mathbf{u}_1$ must be zero. Let $\mathbf{r}_\varepsilon = \mathbf{r}_1 + \mathbf{u}_1\varepsilon$. Then

$$\frac{dg_{11}(\mathbf{r}_\varepsilon)}{d\varepsilon} = (\boldsymbol{\omega}_1 \times \mathbf{u}_1) \cdot (\mathbf{t}_1 \times \mathbf{r}_1) + (\boldsymbol{\omega}_1 \times \mathbf{r}_1) \cdot (\mathbf{t}_1 \times \mathbf{u}_1) + 2\varepsilon(\boldsymbol{\omega}_1 \times \mathbf{u}_1) \cdot (\mathbf{t}_1 \times \mathbf{u}_1) \tag{38}$$

Since (37) holds, $\mathbf{u}_1$ must also satisfy

$$-(\boldsymbol{\omega}_1 \cdot \dot{\mathbf{r}}_1)(\mathbf{u}_1 \cdot \mathbf{t}_1) - (\boldsymbol{\omega}_1 \cdot \mathbf{u}_1)(\mathbf{r}_1 \cdot \mathbf{t}_1) = 0 \tag{39}$$

Thus we obtain

$$\mathbf{u}_1 \cdot ((\boldsymbol{\omega}_1 \cdot \mathbf{r}_1)\mathbf{t}_1 + (\mathbf{t}_1 \cdot \mathbf{r}_1)\boldsymbol{\omega}_1) = 0 \tag{40}$$

We can compute the tangent direction from (40) and (37) as

$$\mathbf{u}_1 = \mathbf{r}_1 \times ((\boldsymbol{\omega}_1 \cdot \mathbf{r}_1)\,\mathbf{t}_1 + (\mathbf{t}_1 \cdot \mathbf{r}_1)\,\boldsymbol{\omega}_1) \tag{41}$$

Similarly, the direction tangent to g_{12} is

$$\mathbf{u}_2 = \mathbf{r}_1 \times ((\boldsymbol{\omega}_1 \cdot \mathbf{r}_1)\,\mathbf{t}_2 + (\mathbf{t}_2 \cdot \mathbf{r}_1)\,\boldsymbol{\omega}_1) \tag{42}$$

Since point $\mathbf{r}_1$ lies on geodesic n, we get

$$\begin{aligned} \mathbf{u}_1 \times \mathbf{u}_2 &= 0 + (\boldsymbol{\omega}_1 \cdot \mathbf{r}_1)(\mathbf{t}_2 \cdot \mathbf{r}_1)((\mathbf{r}_1 \times \mathbf{t}_1) \times (\mathbf{r}_1 \times \boldsymbol{\omega}_1)) + \\ &\quad (\mathbf{t}_1 \cdot \mathbf{r}_1)(\boldsymbol{\omega}_1 \cdot \mathbf{r}_1)((\mathbf{r}_1 \times \boldsymbol{\omega}_1) \times (\mathbf{r}_1 \times \mathbf{t}_2)) + 0 = \\ &= (\boldsymbol{\omega}_1 \cdot \mathbf{r}_1)((\mathbf{t}_2 \cdot \mathbf{r}_1)[\boldsymbol{\omega}_1\,\mathbf{r}_1\,\mathbf{t}_1]\,\mathbf{r}_1 + (\mathbf{t}_1 \cdot \mathbf{r}_1)[\mathbf{t}_2\,\mathbf{r}_1\,\boldsymbol{\omega}_1]\,\mathbf{r}_1) \\ &= (\boldsymbol{\omega}_1 \cdot \mathbf{r}_1)((\mathbf{t}_1 \times \mathbf{t}_2) \cdot (\mathbf{r}_1 \times (\boldsymbol{\omega}_1 \times \mathbf{r}_1)))\,\mathbf{r}_1 \end{aligned} \tag{43}$$

Also

$$\boldsymbol{\omega}_1 \cdot \mathbf{r}_1 = \|\boldsymbol{\omega}_1 \times (\mathbf{t}_1 \times \mathbf{t}_2)\|^2 > 0 \tag{44}$$

and

$$(\mathbf{t}_1 \times \mathbf{t}_2) \cdot (\mathbf{r}_1 \times (\boldsymbol{\omega}_1 \times \mathbf{r}_1)) = [\mathbf{t}_1\,\mathbf{t}_2\,\boldsymbol{\omega}_1]\,\|\boldsymbol{\omega}_1 \times (\mathbf{t}_1 \times \mathbf{t}_2)\|^2\,\|\mathbf{t}_1 \times \mathbf{t}_2\|^2 \neq 0 \tag{45}$$

So $\mathbf{u}_1 \times \mathbf{u}_2$ is not zero, and the two zero motion contours cross at point $\mathbf{r}_1$.

Appendix D Zero motion contour crossing the border of the image

Let the half sphere image be bounded by equator q, let $\mathbf{n}_0$ be a unit vector normal to the plane of q. We would like to know whether the zero motion contour of motion $(\mathbf{t}, \boldsymbol{\omega})$ intersects equator q.

Let us choose a Cartesian coordinate system such that $\mathbf{n}_0 = [0, 0, 1]$. Let $\mathbf{t} = [t_x, t_y, t_z]$ and $\boldsymbol{\omega} = [\omega_x, \omega_y, \omega_z]$. Points on equator q can be written as $[\cos\phi, \sin\phi, 0]$. Thus the zero motion contour $(\boldsymbol{\omega} \times \mathbf{r}) \cdot (\mathbf{t} \times \mathbf{r}) = 0$ intersects q if equation

$$(\omega_x t_x + \omega_z t_z)\sin^2\phi - (\omega_y t_x + \omega_x t_y)\sin\phi\cos\phi + (\omega_y t_y + \omega_z t_z)\cos^2\phi = 0 \tag{46}$$

has a solution.

Writing $\lambda = \tan\phi$, we obtain a quadratic equation

$$(\omega_x t_x + \omega_z t_z)\lambda^2 - (\omega_y t_x + \omega_x t_y)\lambda + (\omega_y t_y + \omega_z t_z) = 0 \tag{47}$$

This equation has a real solution if

$$l = (\omega_y t_x + \omega_x t_y)^2 - 4(\omega_x t_x + \omega_z t_z)(\omega_y t_y + \omega_z t_z) \geq 0 \tag{48}$$

After some manipulation, we obtain

$$\begin{aligned} l &= (\omega_y t_x - \omega_x t_y)^2 - 4(\omega_z t_z)(\omega_x t_x + \omega_y t_y + \omega_z t_z) \\ &= [\mathbf{t}\boldsymbol{\omega}\mathbf{n}_0]^2 - 4(\boldsymbol{\omega}\cdot\mathbf{n}_0)(\mathbf{t}\cdot\mathbf{n}_0)(\boldsymbol{\omega}\cdot\mathbf{t}) \geq 0 \end{aligned} \tag{49}$$

Appendix E Intersections of zero motion contours

Let $(\mathbf{t}_1, \boldsymbol{\omega}_1)$ and $(\mathbf{t}_2, \boldsymbol{\omega}_2)$ be two ambiguous motions. Let us investigate possible intersection points of the zero motion contours of the two motions.

Since ambiguity is possible only when $\boldsymbol{\omega}_1 \times \boldsymbol{\omega}_2 \neq 0$, $\mathbf{t}_1 \times \mathbf{t}_2 \neq 0$, and $(\boldsymbol{\omega}_1 \times \boldsymbol{\omega}_2)\cdot(\mathbf{t}_1 \times \mathbf{t}_2) = 0$, we can choose a Cartesian coordinate system such that

$$\begin{aligned} \hat{X} &= (\boldsymbol{\omega}_1 \times \boldsymbol{\omega}_2)/|\boldsymbol{\omega}_1 \times \boldsymbol{\omega}_2| \\ \hat{Y} &= (\mathbf{t}_1 \times \mathbf{t}_2)/|\mathbf{t}_1 \times \mathbf{t}_2| \\ \hat{Z} &= \hat{X} \times \hat{Y} \end{aligned} \tag{50}$$

In this coordinate system, we can write $\mathbf{t}_1 = [U_1, 0, W_1]$, $\mathbf{t}_2 = [U_2, 0, W_2]$, $\boldsymbol{\omega}_1 = [0, \beta_1, \gamma_1]$, and $\boldsymbol{\omega}_2 = [0, \beta_2, \gamma_2]$.

Clearly, both zero motion contours pass through point $[0, 0, 1]$. We would like to know whether this is the only intersection point.

If W_1 were zero, we would have $\mathbf{t}_1 \cdot \boldsymbol{\omega}_1 = 0$; thus the zero motion contour g_{11} would be degenerate. This is not possible if the motions are ambiguous. Thus $W_1 \neq 0$, and similarly W_2, γ_1, and γ_2 are non-zero.

Since the zero motion contour does not depend on the size (and direction) of vectors $\mathbf{t}$ and $\boldsymbol{\omega}$, we can re-scale vectors $\mathbf{t}_i$, $\boldsymbol{\omega}_i$, multiplying by $\lambda_i \neq 0$ such that

$$\begin{aligned} \hat{\mathbf{t}}_1 &= \lambda_1 \mathbf{t}_1 &&= [\hat{U}_1, 0, 1] \\ \hat{\mathbf{t}}_2 &= \lambda_2 \mathbf{t}_2 &&= [\hat{U}_2, 0, 1] \\ \hat{\boldsymbol{\omega}}_1 &= \lambda_3 \boldsymbol{\omega}_1 &&= [0, \hat{\beta}_1, 1] \\ \hat{\boldsymbol{\omega}}_2 &= \lambda_4 \boldsymbol{\omega}_2 &&= [0, \hat{\beta}_2, 1] \end{aligned} \tag{51}$$

Let us consider point $\mathbf{r} = [x, y, z]$ such that $(\boldsymbol{\omega} \times \mathbf{r}) \cdot (\mathbf{t} \times \mathbf{r}) = 0$. If $z \neq 0$, point $\mathbf{r}/z = [x/z, y/z, 1]$ also satisfies the equation. Thus it is enough to consider two possible sets of points: points of the form $\mathbf{r} = [x, y, 1]$ (i.e., points lying in the plane tangent to the sphere at $[0, 0, 1]$), and points $\mathbf{r} = [x, y, 0]$ (these points correspond to points at infinity on the tangent plane).

A: To obtain the possible intersection points $\mathbf{r} = [x, y, 1]$ we express the zero motion contours as

$$(\hat{\boldsymbol{\omega}}_1 \times \mathbf{r}) \cdot (\hat{\mathbf{t}}_1 \times \mathbf{r}) = x^2 + y^2 - x\hat{U}_1 - y\hat{\beta}_1 - xy\hat{U}_1\hat{\beta}_1 = 0 \tag{52}$$

$$(\hat{\boldsymbol{\omega}}_2 \times \mathbf{r}) \cdot (\hat{\mathbf{t}}_2 \times \mathbf{r}) = x^2 + y^2 - x\hat{U}_2 - y\hat{\beta}_2 - xy\hat{U}_2\hat{\beta}_2 = 0 \tag{53}$$

We can compute y from the difference of the two equations as

$$y = \frac{x(\hat{U}_1 - \hat{U}_2)}{x(\hat{U}_2\hat{\beta}_2 - \hat{U}_1\hat{\beta}_1) + \hat{\beta}_2 - \hat{\beta}_1} \tag{54}$$

Substituting (54) into (52), we obtain a polynomial equation of degree 4 in x. One solution is $x = 0$ (both zero motion contours pass through point $[0, 0, 1]$). The remaining equation of degree 3 has at least one real solution.

If $(\hat{\beta}_1 - \hat{\beta}_2)(\hat{U}_1\hat{\beta}_2 - \hat{U}_2\hat{\beta}_1) = 0$, we obtain another solution $x = 0$. Otherwise the two contours intersect in two different points. Since $\boldsymbol{\omega}_1 \times \boldsymbol{\omega}_2 \neq 0$, we know $\hat{\beta}_1 - \hat{\beta}_2 \neq 0$. Thus the two zero motion contours are tangent only if $\hat{U}_1\hat{\beta}_2 = \hat{U}_2\hat{\beta}_1$. If this is the case, we obtain an equation of degree 2 in x. Its discriminant is

$$d = \hat{\beta}_1^2\hat{U}_1^2(\hat{U}_2 + \hat{U}_1)^2((\hat{U}_2\hat{\beta}_1)^2 - 4) \tag{55}$$

Thus if $|\hat{U}_2\hat{\beta}_1| = |\hat{U}_1\hat{\beta}_2| \geq 2$, the two zero motion contours are tangent at $[0, 0, 1]$, but intersect at two other points.

B: Now we compute intersection points $\mathbf{r} = [x, y, 0]$. We can assume $x^2 + y^2 = 1$. Then we obtain equations $xy\,\hat{U}_1\,\hat{\beta}_1 = 1$ and $xy\,\hat{U}_2\,\hat{\beta}_2 = 1$, so such intersection point exists only if $\hat{U}_1\hat{\beta}_1 = \hat{U}_2\hat{\beta}_2$.

In the previous part we have shown that if $\hat{U}_2\hat{\beta}_1 \neq \hat{U}_1\hat{\beta}_2$, the two zero motion contours have more than one intersection point. So it is enough to check the tangential case here.

If the two contours are tangent at $[0,0,1]$, from $\hat{U}_1\hat{\beta}_1 = \hat{U}_2\hat{\beta}_2$ and $\hat{U}_2\hat{\beta}_1 = \hat{U}_1\hat{\beta}_2$ we obtain $|\hat{U}_1| = |\hat{U}_2|$. Since $\mathbf{t}_1 \times \mathbf{t}_2 \neq 0$, this is possible only if $\hat{U}_1 = -\hat{U}_2$ and $\hat{\beta}_1 = -\hat{\beta}_2$.

Writing $x = \cos\phi$ and $y = \sin\phi$, we obtain equation

$$\sin(2\phi) = -\frac{2}{\hat{U}_1\hat{\beta}_1} = \frac{2}{\hat{U}_1\hat{\beta}_2} \tag{56}$$

so again there is an intersection point if $|\hat{U}_1\hat{\beta}_2| \geq 2$.

Therefore the two zero motion contours have only one intersection point if $\hat{U}_1/\hat{\beta}_1 = \hat{U}_2/\hat{\beta}_2$, and $|\hat{U}_1\hat{\beta}_2| = |\hat{U}_2\hat{\beta}_1| < 2$. If we denote the intersection point of g_{11} and g_{22} as $\mathbf{r}_{12}$, this can be written as

$$\frac{\tan\angle(\mathbf{t}_1, \mathbf{r}_{12})}{\tan\angle(\boldsymbol{\omega}_1, \mathbf{r}_{12})} = \frac{\tan\angle(\mathbf{t}_2, \mathbf{r}_{12})}{\tan\angle(\boldsymbol{\omega}_2, \mathbf{r}_{12})} \tag{57}$$

where $\angle(\cdot,\cdot)$ denotes the angle between two vectors.

This relationship can also be expressed as

$$[\boldsymbol{\omega}_1\boldsymbol{\omega}_2\hat{\mathbf{t}}_1][\mathbf{t}_1\mathbf{t}_2\hat{\boldsymbol{\omega}}_2] = [\boldsymbol{\omega}_1\boldsymbol{\omega}_2\hat{\mathbf{t}}_2][\mathbf{t}_1\mathbf{t}_2\hat{\boldsymbol{\omega}}_1] \tag{58}$$

Furthermore from (55) we obtain the constraint

$$\begin{aligned} &|[\boldsymbol{\omega}_1\boldsymbol{\omega}_2\mathbf{t}_1]\,[\mathbf{t}_1\mathbf{t}_2\boldsymbol{\omega}_2]|\;\|\boldsymbol{\omega}_1 \times \boldsymbol{\omega}_2\|\,\|\mathbf{t}_1 \times \mathbf{t}_2\| < \\ &2\,|(((\boldsymbol{\omega}_1 \times \boldsymbol{\omega}_2) \times (\mathbf{t}_1 \times \mathbf{t}_2)) \cdot \mathbf{t}_1)\,(((\boldsymbol{\omega}_1 \times \boldsymbol{\omega}_2) \times (\mathbf{t}_1 \times \mathbf{t}_2)) \cdot \boldsymbol{\omega}_2)| \end{aligned} \tag{59}$$

Appendix F Antipodal contradictory points

Here for the purpose of providing a description of the areas where two motion fields are ambiguous, the conditions are developed for point $\mathbf{r}$ and its antipodal point $-\mathbf{r}$ both to be contradictory.

Clearly, if one of the CP-conditions holds for $\mathbf{r}$, it cannot be true for $-\mathbf{r}$. So if both $\mathbf{r}$ and $-\mathbf{r}$ are contradictory, two of the conditions must hold at $\mathbf{r}$ and the other two at $-\mathbf{r}$.

If (18) and (19) hold at $\mathbf{r}$ and (20), (21) at $-\mathbf{r}$, we get

$$\mathrm{sgn}(f_t(\mathbf{r})) = \mathrm{sgn}(g_{12}) = -\mathrm{sgn}(g_{22}) = \mathrm{sgn}(g_{21}) = -\mathrm{sgn}(f_\omega(\mathbf{r}))$$

at $\mathbf{r}$ and

$$-\mathrm{sgn}(f_t(\mathbf{r})) = -\mathrm{sgn}(g_{21}) = \mathrm{sgn}(g_{11}) = -\mathrm{sgn}(g_{12}) = \mathrm{sgn}(f_\omega(\mathbf{r}))$$

at $-\mathbf{r}$. Thus

$$\mathrm{sgn}(g_{11}) = \mathrm{sgn}(g_{22}) = -\mathrm{sgn}(g_{12}) = -\mathrm{sgn}(g_{21})$$
$$\mathrm{sgn}(f_t(\mathbf{r})) \neq \mathrm{sgn}(f_\omega(\mathbf{r}))$$

If (18) and (20) hold at $\mathbf{r}$ and (19), (21) at $-\mathbf{r}$, we get $\mathrm{sgn}(g_{12}) = -\mathrm{sgn}(g_{22})$ at $\mathbf{r}$ and $\mathrm{sgn}(g_{12}) = \mathrm{sgn}(g_{22})$ at $-\mathbf{r}$, so this case cannot occur.

If (18) and (21) hold at $\mathbf{r}$ and (19), (20) at $-\mathbf{r}$, we get

$$\mathrm{sgn}(f_t(\mathbf{r})) = \mathrm{sgn}(g_{12}) = -\mathrm{sgn}(g_{22}) = \mathrm{sgn}(f_\omega(\mathbf{r})) = -\mathrm{sgn}(g_{11})$$

at $\mathbf{r}$ and

$$-\mathrm{sgn}(f_\omega(\mathbf{r})) = -\mathrm{sgn}(g_{21}) = \mathrm{sgn}(g_{22}) = -\mathrm{sgn}(f_t(\mathbf{r})) = \mathrm{sgn}(g_{11})$$

at $-\mathbf{r}$. So we get

$$\mathrm{sgn}(g_{11}) = \mathrm{sgn}(g_{22}) = -\mathrm{sgn}(g_{12}) = -\mathrm{sgn}(g_{21})$$
$$\mathrm{sgn}(f_t(\mathbf{r})) = \mathrm{sgn}(f_\omega(\mathbf{r}))$$

Thus point $\mathbf{r}$ and point $-\mathbf{r}$ are both contradictory if and only if

$$\mathrm{sgn}(g_{11}(\mathbf{r})) = \mathrm{sgn}(g_{22}(\mathbf{r})) = -\mathrm{sgn}(g_{12}(\mathbf{r})) = -\mathrm{sgn}(g_{21}(\mathbf{r})) \tag{60}$$

References

[1] N. Ancona and T. Poggio. Optical flow from 1-D correlation: Application to a simple time-to-crash detector. *International Journal of Computer Vision: Special Issue on Qualitative Vision*, 14:131–146, 1995.

[2] O. Faugeras, F. Lustman, and G. Toscani. Motion and structure from motion from point and line matches. In *Proc. International Conference on Computer Vision*, pages 25–34, 1987.

[3] C. Fermüller. Passive navigation as a pattern recognition problem. *International Journal of Computer Vision: Special Issue on Qualitative Vision*, 14:147–158, 1995.

[4] C. Fermüller and Y. Aloimonos. On the geometry of visual correspondence. *International Journal of Computer Vision*, 1995. To appear.

[5] C. Fermüller and Y. Aloimonos. Qualitative egomotion. *International Journal of Computer Vision*, 15:7–29, 1995.

[6] B. Horn. Motion fields are hardly ever ambiguous. *International Journal of Computer Vision*, 1:259–274, 1987.

[7] B. Horn. Relative orientation. *International Journal of Computer Vision*, 4:59–78, 1990.

[8] H. Longuet-Higgins. A computer algorithm for reconstruction of a scene from two projections. *Nature*, 293:133–135, 1981.

[9] S. Maybank. *Theory of Reconstruction from Image Motion.* Springer, Berlin, 1993.

[10] S. Negahdaripour. Critical surface pairs and triplets. *International Journal of Computer Vision*, 3:293–312, 1989.

[11] S. Negahdaripour and B. Horn. Direct passive navigation. *IEEE Transactions on Pattern Analysis and Machine Intelligence*, 9:163–176, 1987.

[12] M. Spetsakis and J. Aloimonos. Structure from motion using line correspondences. *International Journal of Computer Vision*, 1:171–183, 1990.

[13] M. Tistarelli and G. Sandini. Dynamic aspects in active vision. *CVGIP: Image Understanding: Special Issue on Purposive, Qualitative, Active Vision*, 56:108–129, 1992.

[14] R. Tsai and T. Huang. Uniqueness and estimation of three–dimensional motion parameters of rigid objects with curved surfaces. *IEEE Transactions on Pattern Analysis and Machine Intelligence*, 6:13–27, 1984.

[15] T. Vieville and O. D. Faugeras. Robust and fast computation of edge characteristics in image sequences. *International Journal of Computer Vision*, 13:153–179, 1994.